HIGH PERFORMANCE LIQUID CHROMATOGRAPHY WITH TANDEM LASER INDUCED FLUORESCENCE AND MASS SPECTROMETRY DETECTION METHODS TO MONITOR THE METABOLIC PROFILE OF DOXORUBICIN AND ITS ALTERATION WITH AGE

A DISSERTATION SUBMITTED TO THE FACULTY OF THE GRADUATE SCHOOL OF THE UNIVERSITY OF MINNESOTA

BY

JOSEPH BRADLY KATZENMEYER

IN PARTIAL FULFILLMENT OF THE REQUIREMENTS FOR THE DEGREE OF

DOCTOR OF PHILOSOPHY

EDGAR A. ARRIAGA, ADVISOR

SEPTEMBER, 2010

Acknowledgements

A scientific research project of this magnitude cannot be carried out without the assistance of others. First and foremost, I must thank Professor Edgar Arriaga for his dedication and guidance along my academic path. His support during my time at the University made this journey both memorable and valuable. All members of Professor Edgar Arriaga's research group during my time at the University of Minnesota played a role in learning and advancing this research project as well as many other experiences not directly represented in this thesis. Post-doctoral associate Dr. Christopher Eddy began the setup of HPLC-LIF and initial mass spectrometry work on doxorubicin within our research group. His experience gave me a starting point to continue the research in this area. Assistance with the interface and method development for HPLC-MS work was received from both Drs. Dana Reed and Joe Dalluge, Directors of the University of Minnesota Chemistry Department Mass Spectrometry Facility. This project could not have progressed efficiently without their valuable advice, guidance and support. The research presented in this thesis also had the fortunate support of the NIH training grant Functional Proteomics in Aging, T32-AG029796.

Lastly, and certainly not least, this work could not have been accomplished without the loving support of my friends and family, specifically: my wife, Melissa, and my mother, Janelle.

Dedication

This work is dedicated to my father, Bradly Joseph Katzenmeyer, without whom I would not be where I am today.

Abstract

In this thesis, a combination of high-performance liquid chromatography (HPLC), laser-induced fluorescence (LIF) and mass spectrometry (MS) is used to assess the metabolic profile of doxorubicin *in vitro* using the post-mitochondrial fraction (PMF) from the liver of Fischer 344 rats. Monitoring the metabolism of xenobiotics and drugs is important in the development, screening and assessment of new chemical compounds for use in therapies. This often requires the use of two or more techniques in order to collect the relevant data. This is the case for the analysis of metabolic products of the anticancer drug doxorubicin.

An HPLC instrument with tandem LIF and MS detection was developed and then used to quantify and identify the metabolic products of doxorubicin *in vitro*. Using this instrumentation, the consumption of doxorubicin and the appearance of 7-deoxydoxorubicinone and 7-deoxydoxorubicinolone were monitored in rat liver post-mitochondrial fractions. This application demonstrates the potential of the tandem LIF-MS detection scheme in quantification and characterization of biotransformations of fluorescent xenobiotics of biomedical and environmental relevance.

The HPLC-LIF-MS instrumentation and *in vitro* methods were then applied to investigate the changes in metabolism between young adult (10 months-old, 100% survival rate) and old (26 months-old, ~25% survival rate) Fischer 344 rats. Results suggest that with aging there is decrease in the rate of biotransformation of doxorubicin and that the timeframes needed to reach steady metabolite and doxorubicin levels are

longer. On the other hand, the levels of metabolites and doxorubicin concentrations are not statistically different between the two age groups.

In the future, the new methodologies presented here could be applied to investigate age-related changes in metabolism of drugs already in use, new compounds and xenobiotics with health relevance (e.g. pesticides or environmental pollutants).

Table of Contents

List of Tables

Chapter 2

Chapter 3

List of figures

Chapter 2

Chapter 3

Chapter 4

Appendix A

Appendix B

List of Abbreviations

ADME: Absorption, distribution, metabolism and excretion

CE: Capillary electrophoresis

CE-MS: Capillary electrophoresis with mass spectrometry detection

CYP450: Cytochrome P450

DC: Direct current

DMSO: Dimethyl sulfoxide

ESI-MS: Electrospray ionization-mass spectrometry

FWHM: Full width at half maximum

HPLC: High-performance liquid chromatography

ICR: Ion cyclotron resonance

LIF: Laser-induced fluorescence

m/z: Mass to charge ratio

MEKC-LIF: Micellar electrokinetic chromatography with laser-induce fluorescence detection

MS: Mass spectrometry

PMF: Post-mitochondrial fraction

Q-TOF: Quadrupole-time of flight

rf: Radio frequency

RPLC: Reverse-phase liquid chromatography

SPE: solid-phase extraction

TLC: Thin-layer chromatography

TOF: Time of flight

TRIS: Tris(hydroxymethyl)aminomethane

Chapter 1

Introduction

Xenobiotics are defined as chemical compounds that are foreign to the biological system. They can include natural compounds, environmental agents, carcinogens, insecticides, plant constituents, drugs, pesticides, cosmetics, flavorings, fragrances, food additives, industrial chemicals and environmental pollutants. It has been estimated that humans are exposed to 1-3 million xenobiotics in their lifetimes [1, 2]. Most of these chemicals, after they gain access to the body through diet, air, drinking water, drug administration, and lifestyle choices, undergo a broad range of processes of detoxification that in general render them less toxic, more polar, and readily excreted [2]. In pharmacokinetics the acronym ADME (absorption, distribution, metabolism and excretion) is used to describe the processes acting on a drug within an organism. Each of the four criteria can affect the drug's concentration and kinetics within the body.

Phase I metabolism involves oxidation and/or reduction in order to detoxify and eliminate the xenobiotics from the body. The rate of phase I metabolism is an important consideration in determining the half-life and the steady state concentration of a compound within the body. One of the largest and most diverse superfamilies of metabolizing enzymes in phase I metabolism is the cytochrome P450 (CYP450) [3]. In previous studies, the expression and activity of the CYP450 enzymes was shown to decrease with age in rat models [4-6]. These studies were highly relevant to research on drug treatments administered to the older population which is more susceptible to prolonged exposure to a drug or foreign compound and drug-drug interactions [7]. New methodologies to quantify and identify metabolites are needed to investigate age-related changes in metabolism and to screen drugs and xenobiotics. The goals of this thesis are to describe new methods of analysis for monitoring the metabolism profile of drugs and

xenobiotics and how the metabolism profile changes with age of an organism. In this thesis, doxorubicin is chosen as a model drug to develop new bioanalytical tools to accomplish the quantification and identification of metabolite compounds.

Chapter 2 gives the reader necessary background information for the work presented in this thesis. Chapter 3 introduces a new combination of high-performance liquid chromatography (HPLC) with tandem laser-induced fluorescence (LIF) and mass spectrometry (MS) detectors for the investigation of the metabolic profile of doxorubicin in a model *in vitro* system. Two metabolite compounds, 7-deoxydoxorubicinolone and 7-deoxydoxorubicinone, were observed and profiled over the course of a one hour *in vitro* incubation. The fluorescence detector provided quantitative data to calculate concentrations of each compound while the mass spectrometry data provided a means of identifying each compound. Chapter 4 describes the use of HPLC-LIF-MS methodology in the exploration of changes in metabolic profiles with age; a comparison is made between 10 months-old and 26 months-old Fischer 344 rats. The timeframes of reaching a steady-state concentration in the metabolism system and the maximum initial rate of biotransformations were both observed to be significantly slower in the old rat age group. Chapter 5 summarizes the current status of this project and outlines applications for future studies in advancing the instrumental applications and aging research. Particularly, it highlights that the techniques presented here could be easily adaptable and be used routinely for the analysis of xenobiotics in biological systems, investigation of different metabolic properties of different organs or tissues and also further the research into metabolism amongst multiple age groups.

Chapter 2

Background

2.1. Drugs and Xenobiotics

Drugs are xenobiotic compounds often administered orally, intravenously, topically, etc. to a patient in order to remedy a disease. Once such compounds enter the biological system, whether human, animal model or cell, the compounds are exposed to a wide range of chemical environments [8-10]. In these environments, there are multiple enzymes (i.e. esterases, amine oxidases, cytochrome P450s, etc.) responsible for the metabolic reactions experienced by the xenobiotic compounds [4, 8, 11, 12]. It is difficult to predict all of the biotransformations that may take place as a chemical compound enters and travels through the body. Understanding the chemical changes a compound experiences is the key to predicting any desired effects or undesired side effects caused by a given drug treatment. Development of sensitive tools and techniques, such as those described in this thesis, would enable the screening and assessment of drugs and xenobiotics and their metabolites in diverse organs and tissues which ultimately furthers our understanding of the roles that such biotransformations play in modern medicine.

2.2. Metabolism

2.2.1. Organs of Interest

Important organs in metabolic studies are the liver, small intestine and the kidney. The liver plays a major role in the metabolism and excretion of xenobiotics [13]. However, the small intestine also contains a number of drug metabolizing enzymes [9]. Kidney also has an impact on drug metabolism, even when the metabolized drugs are not eliminated renally [14]. Each one of these organs presents a unique chemical environment to a xenobiotic compound because they contain different types and amounts of metabolic enzymes [8, 9, 15]. Since liver tissue is highly abundant in CYP450

enzymes, it can be used to develop a drug metabolism model. In this work, liver tissue was used because it plays a major role in drug metabolism and was expected to produce relevant and abundant metabolites.

2.2.2. Metabolism of Xenobiotics

Metabolism makes foreign compounds more hydrophilic and more easily excreted from the body. Phase I metabolism includes the structural modification of the xenobiotic through oxidation, reduction or hydrolysis [13]. This is followed by phase II metabolism which refers to conjugation reactions of a compound with a chemical ligand such as glucuronide, sulphate, acetate or glutathione. This is followed by excretion of the detoxified compounds [13].

The largest and most functionally diverse superfamily of metabolizing enzymes is the cytochrome P450s (CYP450s) [16]. The functions of these hemoproteins include phase I drug metabolism, steroidogenesis, and the metabolism of fatty acids [3]. There are in excess of 2000 identified CYP450s grouped into 265 families. Humans have 75 individual CYP450s [3]. CYP450s can be found embedded in the endoplasmic reticulum (microsomal type, most common), in the mitochondria or in the cytosol [3]. CYP families 1, 2, and 3 are responsible for drug metabolism and have a multitude of substrates, inhibitors and inducers. These three families alone are composed of 17 subfamilies. CYP 1A1, 1A2, 3A4, 3A5 and 3A6 are specific CYPs shown to be induced and inhibited by doxorubicin the model drug used for the work described in this thesis [3, 17].

2.2.3. Aging and Metabolism

According to the United Nations, the world population has been growing older steadily since about 1950 [18]. In 2009, 11% of the population was reported to be greater than or equal to 60 years old; this is projected to increase to 22% by 2050 [18]. In addition, the elderly population takes more medications than other age groups. In a survey, 81% of women over the age of 65 took at least one prescription medication and 23% took at least 5 in the preceding week [19]. In that same study, 12% of women over the age of 65 took at least 10 medications (prescription and OTC) in the preceding week. Another study of nursing home residents reported that 39.5% of female residents took greater than or equal to 9 medications [20]. With the large number of medications taken by the elderly population, there is an increased risk of adverse drug reactions. A higher risk of drug-drug interactions has been linked to age in addition to the number of medications taken [7]. Inhibition of metabolism is an increasingly significant explanation for the adverse drug-drug interactions [7].

The factors included in ADME (absorption, distribution, metabolism and excretion) have all been reported to have age-related changes [21]. Specifically, metabolism is affected by decreased liver volume and blood flow [13, 21]. This reduces the efficiency of CYP450-mediated phase I metabolism in the liver [21]. It has even been suggested that the dosage given to elderly patients be reduced by 30-40% from what is administered to middle-aged patients to take into account reduced liver and renal function [13]. Studies using human subjects have been performed to examine metabolism changes with age [5]. Here, a 30% decrease in both *in vivo* and *in vitro* metabolism of antipyrine

by cytochrome P450 enzymes was reported after 70 years of age. This decline began after 40 years of age.

Previous research in animals has suggested a decline in metabolism with age. Age-related changes in enzymatic metabolism or clearance of a xenobiotic compound or drug are difficult to measure [22]. Lee, *et al*. found that in Brown Norway rats the expression of CYP2B2, a xenobiotic metabolizing enzyme, and glutathione-S-transferase decreased with age [4]. They suggest that low metabolic activity would increase the rat's susceptibility to certain classes of compounds with aging. A second study using rats as models to examine changes in cytochrome P450 enzymes with age reports an age-related decrease in metabolizing enzymes. Wauthier, et al., studied the effect of aging on CYP450 enzymes in Wistar rats. Observations showed that main CYP450 enzymes (i.e. CYP2C11 and CYP3A2) decreased significantly with age [6]. Bolling, et al., studied glucuronidation (a phase II metabolism process) by rat liver microsomes [23]. In Fischer 344 rats, the glucuronidation of quercitin was reduced with increased age of the rat.

There is a need to understand how drugs and xenobiotics affect different age groups including: young, middle-aged and elderly [5]. Elderly patients are more susceptible to drug-drug interactions [7]. In order to improve treatment of age groups susceptible to complications with foreign compounds, methods and technologies are needed to assess the change in metabolism with age.

2.3. Anthracyclines

2.3.1. Properties

Anthracyclines are synthetic or naturally occurring compounds with antitumor properties. These compounds have two characteristic structural features: a multi-ring semi-quinone structure as a backbone and a sugar moiety (daunosamine) [24]. Figure 2-1 is the structure of doxorubicin that was used as a drug model in this work. Other members of this compound class that have demonstrated efficacy in the treatment of many types of cancer (e.g. sarcomas, carcinomas and lymphomas) including both solid tumors as well as leukemia are daunorubicin, idarubicin, and amrubicin [25-27]. Doxorubicin is administered under the trade names Adriamycin, Rubex and Doxil (a liposomal formulation) [18].

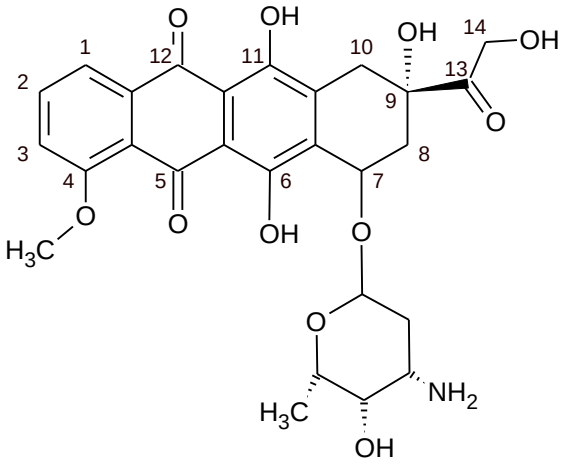

Figure 2-1. Structure of the common anthracycline doxorubicin. Carbons 13 and 7 are most commonly modified during metabolism.

Doxorubicin has a major drawback, however, in the form of cumulative cardiotoxicity. It is still uncertain, however, as to the exact cause of this cardiotoxicity. For example, doxorubicin can cause damage through the production of reactive oxygen species. The quinone substructure of doxorubicin allows it to accept electrons mediated by P450 reductase, NADH dehydrogenase, and xanthine oxidase [25]. These reactive semiquinones can then go on to cause free-radical damage to DNA itself or react with molecular oxygen to form superoxide, hydroxyl radicals, and peroxides that can cause

damage [25]. Production of reactive oxygen species may play a role in the cardiotoxic effects. The drastic side-effect of cardiotoxicity caused by a metabolism product of doxorubicin illustrates the need to observe the metabolic fate of drugs upon entering the body.

2.3.2. Metabolism of Doxorubicin

Most of the doxorubicin metabolism appears to occur intracellularly [24]. However, some changes may occur in biofluids, such as plasma, urine and bile [24].

The earliest studies of metabolism of doxorubicin reported seven possible metabolites (Figure 2-2) [10, 24, 28]. CYP450s can act on doxorubicin causing carbonyl reduction as well as oxidative or reductive cleavage of the daunosamine sugar moiety [29].Carbon number 13 (Figure 2-1) is susceptible to reduction to produce doxorubicinol (Figure 2-2, II). This is the most commonly studied and reported metabolite of doxorubicin and has been linked to doxorubicin's cardiotoxic side-effects. The daunosamine sugar moiety can also be cleaved from the parent drug. This produces a set of metabolites known as the aglycone metabolites. This process can either proceed through a hydrolase-type deglycosidation to form doxorubicinone (Figure 2-2, III) or a reductase-type deglycosidation to produce 7-deoxydoxorubicinone (Figure 2-2, V) and 7-deoxydoxorubicinolone (Figure 2-2, VI). This knowledge on the types of metabolite compounds that are expected to be observed makes doxorubicin a useful drug model in development of techniques to observe metabolism and age-related effects on metabolism.

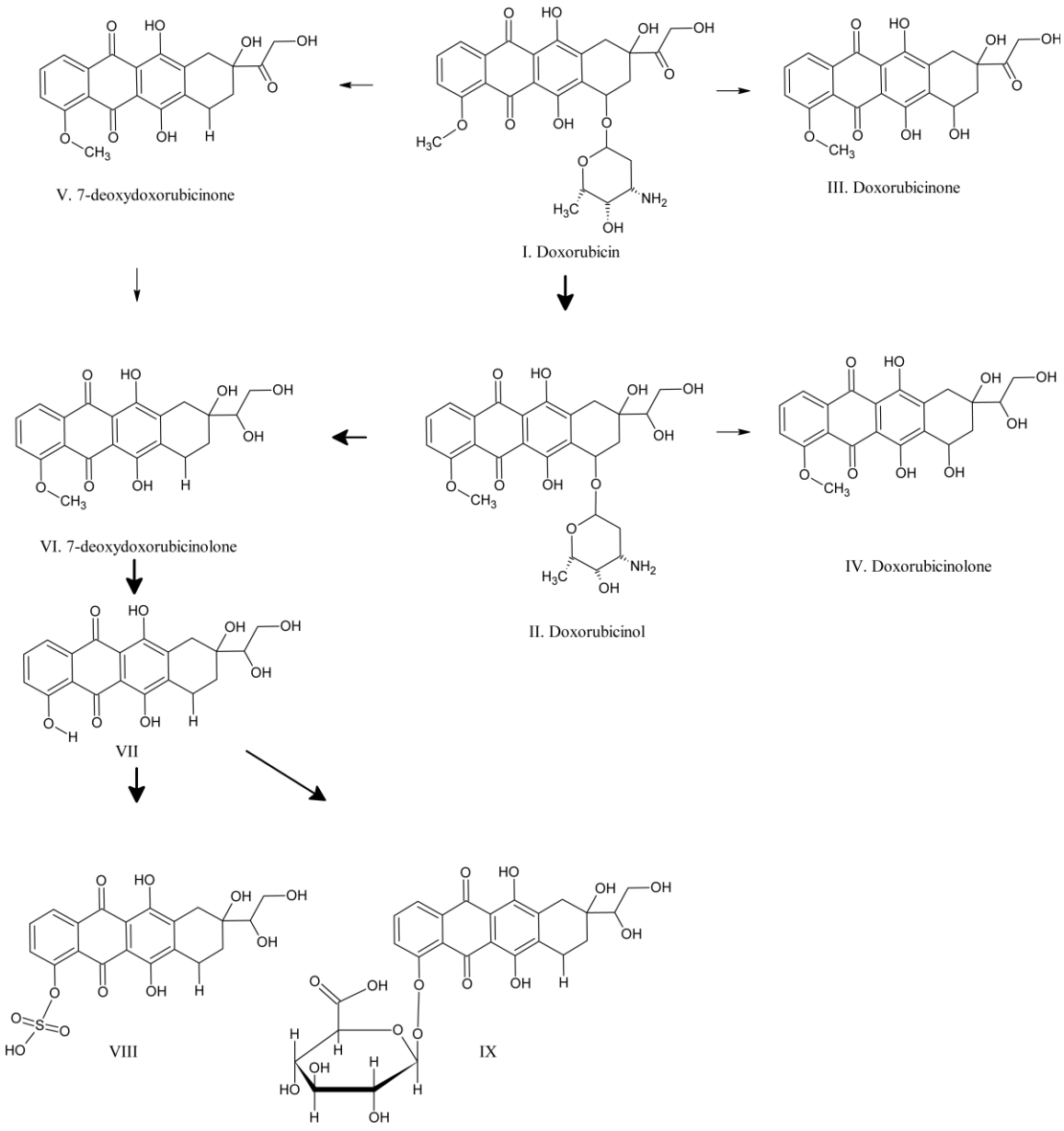

Figure 2-2. Metabolic scheme of doxorubicin. Metabolites I-VI are most commonly observed phase I metabolites. Numbers VII – IX are phase II metabolites (See section 2.2.2). Larger arrows represent preferred metabolic routes [28].

2.4. High-Performance Liquid Chromatography (HPLC)

Reversed phase liquid chromatography (RPLC) is a separation mode of HPLC based on the solvophobicity of analyte molecules and their thermodynamic partitioning between the mobile and stationary phases [30]. In this partitioning mechanism solutes associate with and dissociate from the stationary phase, which is typically made of C18 or C8 alkyl chains [31, 32]. In practical terms, if an analyte and the stationary phase are more similar in chemical structure, intermolecular forces will favor the analyte being associated with the stationary phase [32]. Those compounds that are favored in the stationary phase will move more slowly through the column. For the compounds shown in Figure 2-2, doxorubicin (I) and doxorubicinol (II) would tend to elute from the column earliest; the sugar moiety interact well with the aqueous mobile phase. The aglycone metabolites (III-VII) tend to be more hydrophobic and elute at a later time from the column.

Separation of small-volume samples by HPLC are performed better in columns of reduced diameter (less than 0.5 mm inner diameter) than in standard HPLC column (4.6 mm diameter) due to the reduction in chromatographic dilution. Chromatographic dilution is dependent on the radius of the column and is caused by small amounts of analyte partitioning into a larger volume of mobile phase [33-35]. Columns with dimensions of 0.3-0.5 mm (μHPLC) and 10-100 μm (nano-HPLC) are used to reduce the effect of chromatographic distribution. In metabolic studies low sample volumes are common and the lowest possible detection limit is desirable to observe low level metabolites. This thesis describes the use of μHPLC (column diameter 0.3 mm) to separate and observe low level metabolites.

In order to compare and evaluate μHPLC separations of primary drugs and their metabolic products, the following parameters are considered and used throughout this thesis: retention factor, number of theoretical plates, and resolution. The retention factor (k') is directly related to the thermodynamic distribution coefficient (K) by the volume ratio of stationary and mobile phases (V_s/V_m). Therefore, when all conditions (i.e. column, mobile phase composition and instrument) are kept constant, k' is a constant for a given compound. In addition, k' can be experimentally determined from the retention time (t_r) of a compound and the elution time of unretained compounds (dead time, t_m) as:

$$k' = K\frac{V_s}{V_m} = \frac{t_r - t_m}{t_m} \tag{2-1}$$

The number of theoretical plates (N) can be used to characterize the efficiency of the system. Each plate represents a region of the column where a local equilibrium occurs. Analogous to the distillation theory from which plate theory is derived, a higher number of plates is indicative of a higher number of equilibrium zones and higher separation capacity of the given set of conditions. N is calculated using Equations 2-2

$$N = 5.54\left(\frac{t_r}{w_{1/2}}\right)^2 \tag{2-2}$$

where $w_{1/2}$ is the width of the peak at half of the height and L is the length of the column.

Resolution is a measure of the separation between two adjacent peaks (e.g. peaks 1 and 2) in a chromatogram. Resolution values are calculated using Equation 2-3. The parameters $t_{r,2}$ and $w_{1/2,2}$ are the retention time and the width of the peak at half height, respectively, for peak 2. The same is true for peak one.

$$R_s = 1.176 \frac{t_{r2} - t_{r1}}{w_{1/2_1} + w_{1/2_2}} \qquad (2\text{-}3)$$

Two chromatographic peaks are resolved to the baseline when R_s is equal to or greater than 1.5.

This thesis work used k', N, and R_s to assess, modify and compare chromatographic separations and then select a suitable separation method used to observe doxorubicin and its metabolites.

2.5. Fluorescence Detection of Anticancer Drugs

Fluorescence detection has become an important tool in the analysis of anticancer drugs [36]. Because of the presence of aromatic and/or heterocyclic rings in their molecular structure, a number of anti-cancer drugs display strong, native fluorescence upon one-photon or multi-photon excitation (Table 2-1) [36]. Due to the conjugated ring structure of doxorubicin, it exhibits a native fluorescence with an absorption maximum at about 500 nm and an emission maximum at about 580 nm (Figure 2-3) [37]. This allows the use of fluorescence detectors in many sensitive analyses of doxorubicin. Fluorescent detection offers excellent analytical performance in terms of sensitivity, selectivity, concentration range and applicability to a number of biomedically-important substances, including doxorubicin. Applications of fluorescence detection include: (i)

Table 2-1. Fluorescence emission maxima of selected anticancer drugs [36].

Anticancer Drug	λ_{em}
Camptothecin	420, 428 nm
Topotecan	538 nm
Pazelliptine	440 nm
9-Aminoacridine	480 nm
Doxorubicin	590 nm
Dipyridimole	500 nm

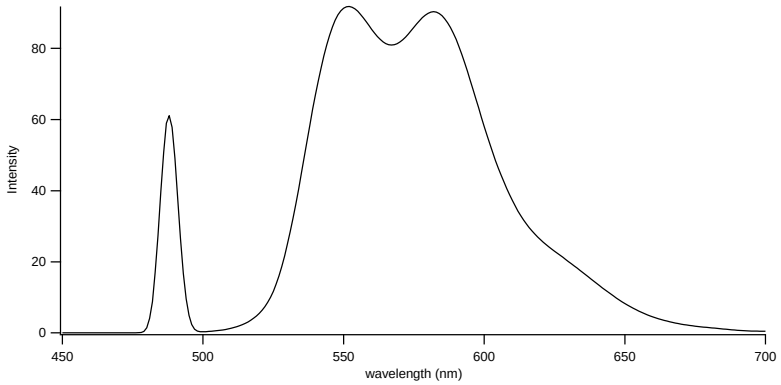

Figure 2-3. Fluorescent emission of Doxorubicin when excited with 488 nm light. The signal at 488 nm corresponds to unfiltered excitation light.

fluorescence microscopy, (ii) fluorescence spectroscopy and (iii) laser-induced fluorescence (LIF).

Fluorescence microscopy technologies have been widely developed in order to localize anticancer drugs in cells and to monitor the possible intracellular changes of these drugs [36]. Confocal fluorescence microscopy suggests that doxorubicin accumulates in the nucleus, Golgi apparatus, lysosomes, mitochondria, cytoplasm, and microtubule network [38-40]. However, the metabolites of doxorubicin are also fluorescent and cannot be distinguished from one another by microscopy.

Fluorescence spectroscopy has been used in the observation of doxorubicin and metabolites [10, 28, 41]. Spectroscopic analysis is performed after a separation method, typically thin-layer chromatography (TLC) in order to identify and quantify the fluorescent species [10, 28]. However, these experiments require large amounts of sample. Takanashi, *et al.* used human urine collected for five days in order to have sufficient amounts of metabolites for their TLC studies [28]. A preconcentration was performed using Silicic acid column chromatography.

Laser-induced fluorescence (LIF) detection has been used to monitor metabolic profiles of doxorubicin in cell cultures [37, 42] and subcellular fractions [43]. Using micellar electrokinetic chromatography (MEKC, a mode of capillary electrophoresis) with LIF detection, doxorubicin was observed on a single cell level [37]. Fluorescence detectors have also been combined with HPLC in order to accomplish the detection of doxorubicin and its metabolites [44, 45]. A detection limit of 61±13 zmol of doxorubicin was reported [37]. Therefore, LIF was chosen in order to conduct quantification of doxorubicin and metabolites throughout the work reported in this thesis.

2.6. Mass Spectrometry

2.6.1. Electrospray Ionization

Mass spectrometry provides structural data that is useful in identification of unknown compounds within a given sample. Two modes of detection are possible with mass spectrometers; positive and negative ions. The protonated $[M+H]^+$ ion, sodium and potassium adducts are commonly observed in detection of positive ions. In negative ion mode, deprotonated ions are typically observed.

Electrospray ionization combined with mass spectrometry (ESI-MS) is currently used for qualitative and quantitative studies of a wide variety of nonvolatile and thermally labile simple inorganic chemicals as well as complex biological structures [46]. ESI-MS is used for the determination of the mass to charge ratio (m/z) of chemical species. This technique is easily interfaced with HPLC systems thereby collecting mass spectra while compounds elute from the chromatographic column. μHPLC systems interface well with ESI-MS because their flow rates are highly compatible. Typically a suitable flow rate for

ESI is 3-5 µL/min, while a µHPLC instrument is commonly operated at a flow rate of 3.5 µL/min.

As shown in Figure 2-4, the outlet of the HPLC instrument is connected directly to the inlet port of the ESI source. The inlet capillary of the ESI source is held at a potential of 2-5 kV relative to a metal plate. The high potential difference causes the solution entering the source to be charged and the liquid begins to migrate towards the metal plate forming what is known as the Taylor cone [47]. From the end of the cone charged droplets of the solution detach and progress towards the metal plate and as the solvent in the droplets evaporate, the droplets fragment into increasingly smaller droplets, due to coulombic repulsion of the excess charge, until what is left is charged analyte molecules [48, 49]. The droplet formation and the desolvation of the analyte molecules is often aided by a flow of an inert sheath gas [47]. The resulting ions accelerated by the metal plate counter electrode, then pass into a mass analyzer.

The major concern of the use of ESI-MS in combination with µHPLC is the compatibility of the HPLC mobile phase with ESI. There are a number of factors that influence the ionization (and detection) of the compounds of interest: (i) pH, (ii) electrospray stability, and (iii) interfering ions.

An acidic pH benefits the ionization process of basic molecules when using positive ion mode [47]. Also, it has been observed that deprotonated ions of acidic groups (negative ions) can be observed even under acidic conditions [47]. Indeed, acidic conditions aid in the suppression of background ions when detecting negative ions lowering the background signal. Therefore, the acidic conditions are suitable, and

preferred, even if unknown compounds are deprotonated at the working pH. The addition of 0.1% formic acid in the aqueous component of the mobile phase was used to adjust the pH and assist in ionization in the analysis of doxorubicin and metabolites described in Chapters 3 and 4.

Stability of the electrospray is essential to obtain reproducible spectra. A content of around 50% polar organic solvent such as methanol or acetonitrile aids in the formation of a stable electrospray. Because these organic solvents decrease the surface tension of the solution, formation of small, stable droplets is favored (Figure 2-4) [47]. The use of the sheath gas reduces the dependence on surface tension by aiding in the formation of droplets by promoting the evaporation of the mobile phase components [47]. In the experiments described in Chapters 3 and 4, acetonitrile is used in the mobile phase

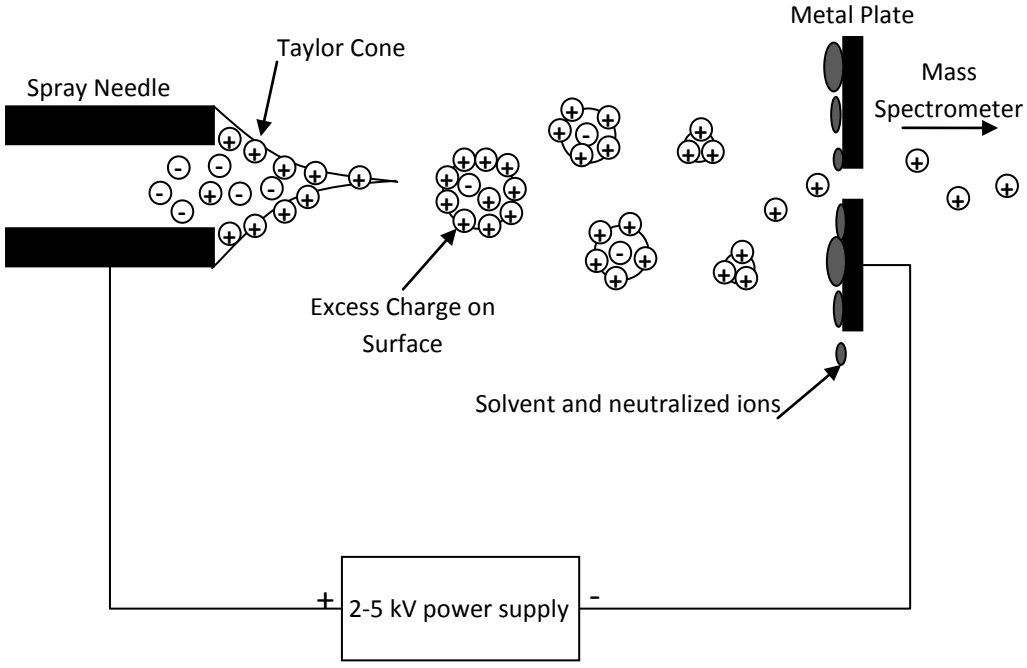

Figure 2-4. Diagram of electrospray ion source [47].

for analysis. In addition, a sheath flow of warm nitrogen was used to assist in the evaporation of solvent molecules.

The ionic contents of the electrosprayed solution influence the ionization process. Since there is a finite amount of current that can flow between the electrospray tip and the counter-electrode, the presence of any carrier of charge will decrease the ionization of the analyte (Figure 2-4) [50]. Ionization suppression due to the presence of non-volatile components in the mixture, such as sulfates and phosphates, is a common problem [50]. Ammonium formate and ammonium acetate are often used in HPLC-MS and CE-MS experiments due to their higher volatility over other additives in order to adjust the pH of the mobile phase [47]. However, at high concentrations, even these volatile components reduce the ionization efficiency [47]. In the work presented in this thesis, low concentrations of formic acid (0.1%) were used in the HPLC mobile phase which is volatile enough to avoid interference with ionization.

Quantification can be performed using ESI-MS. However, the use of an internal standard is necessary as MS detectors are not as stable and robust as conventional detectors [51]. Co-eluting compounds can deteriorate (suppress or enhance) the ionization of the analyte and/or the internal standard [51]. While internal standards should mimic closely the analyte of interest, it is not the same compound and will add complexity to an already complex mixture. The use of stable, isotopically-labeled compounds as internal standards is the ideal situation. The standard and analyte would be equally affected by any change in ionization efficiency [51]. However, stable isotopes are not always readily available and may be rather expensive.

2.6.2. Mass Analyzers

Multiple types of mass analyzers are widely used in mass spectrometers in order to detect and report the mass to charge ratio (m/z) of ions entering the instrument, namely, quadrupole, quadrupole ion trap, ion cyclotron resonance (ICR), Orbitrap and time of flight (TOF) mass analyzers [46, 52]. These analyzers (Table 2-2) vary in terms of size, price, resolution, mass range, and the ability to perform tandem mass spectrometry experiments (MS/MS) [46]. Only those used in the study of doxorubicin metabolism in Chapters 3 and 4 are discussed below.

Quadrupole mass analyzers are essentially four parallel metal rods. Two of the metal rods have a direct current potential (U) applied while the remaining two rods are linked to an alternating radio-frequency (rf) potential (V) [46]. Under appropriate conditions of U, V and rf, only ions within a narrow range of m/z will survive the path toward the detector [46]. The quadrupole acts as an m/z filter and by scanning values of U, V and rf the spectrum of m/z values can be passed to an ion detector. Benefits of a quadrupole analyzer are low cost, robustness and ease of maintenance [46]. Drawbacks of using a quadrupole mass analyzer are a limited mass range (m/z <4000) and low mass resolution,

Table 2-2. Selected mass spectrometry detectors [46, 52].

Detector	Benefits	Drawbacks
Quadrupole	Low cost, easy maintenance	Limited mass range, low mass resolution
Quadrupole Ion Trap	MS^n experiments possible	Limited mass range, low mass resolution
Ion Cyclotron Resonance	High mass accuracy and resolution	High field magnet, size and cost
Orbitrap	Higher sensitivity	High vacuum
Time-of-Flight	High mass resolution, unlimited mass range	Size, resolution depends on length of flight tube

usually unit resolution [46, 53].

The time-of-flight (TOF) mass analyzer is based on the time of free flight of the ion through a drift tube [46, 53]. A direct relationship is observed between the m/z value and the time of flight. Correlates m/z with total time of flight (t_f) is expressed in the following formula:

$$m/z = \frac{t_f^2 2Es}{(2s + x)} \tag{2-4}$$

where E is the voltage applied, s is the length of the ion acceleration region, and x is the length of the free flight region. Theoretically E, s, and x are fixed; therefore, the above equation can be reduced to:

$$m/z = Kt_f^2 \tag{2-5}$$

where K is the calibrating factor. This equation illustrates the direct relationship between the m/z value and the time of flight. Extending the length of the free flight region of the analyzer increases the mass resolution of the instrument. Because ions entering the TOF carry different kinetic energies, this can adversely affect the resolution of the m/z values [46, 53]. This is overcome with the addition of a reflectron (electrostatic mirror) [46, 53, 54]. Benefits of using a TOF detector are that (i) all ions reach the detector, (ii) superior mass resolution and (iii) a theoretically unlimited mass range [46, 55].

The combination of a quadrupole and TOF (Q-TOF) mass analyzers is adequate to perform tandem MS (MS/MS) experiments to collect more structurally relevant data [46].

The use of a Q-TOF instrument combines the mass scanning capabilities of the quadrupole with the resolving power of the TOF mass analyzer [46]. The quadrupole can act as a mass filter allowing specific ions into a collision cell where they are fragmented by collision induced dissociation. The accurate masses of the fragments are then determined by the TOF mass analyzer [46]. A Q-TOF instrument is limited to MS/MS instruments whereas other mass analyzers (e.g. ICR and Orbitrap) can conduct MS^n experiments with multiple fragmentation steps. However, in experiments with multiple possible components, it is more beneficial to detect as many compounds as possible instead of dwelling on fragment ions of one compound.

The Bruker MicrOTOF$_Q$ mass spectrometer is a Q-TOF instrument with an orthogonal acceleration TOF analyzer and a reflectron. This instrument routinely collects spectra with 10,000 to 11,000 mass resolution (full width at half maximum (FWHM) of the m/z peak compared to m/z, Equation 2-6), ~0.2 mDa precision, and tolerances (difference between calculated, m_{calc}, and observed mass, m_{obs}, Equation 2-7) ~ 10 ppm,

$$\text{Mass Resolution} = \frac{m/z}{FWHM} \tag{2-6}$$

$$\text{Mass Tolerance} = \frac{|m_{calc} - m_{obs}|}{m_{obs}} \tag{2-7}$$

which are adequate to generate an initial list of possible chemical compositions when the goal is to identify an unknown compound. Unfortunately, this list still has many possible chemical formulas for each observed mass. For example, a compound with m/z of 400 and a 10 ppm mass tolerance would be expected to generate 50-60 elemental compositions containing C, H, N, O and S [56]. The pattern and intensities of the isotope

peaks help reduce this list of possible chemical compositions. This is referred to as a sigma value within the Bruker DataAnalysis software package. In many cases, the sigma value is a better representation of the fit of a chemical composition than the mass error.

2.6.3. Mass spectrometry of Doxorubicin

Mass spectrometry has been used to identify anthracyclines and their metabolites [57, 58]. An m/z of 544 is characteristic of doxorubicin. An aglycone fragment of m/z 397 is also observed for doxorubicin. This ion is indicative of the loss of the daunosamine sugar moiety (Figure 2-1). The daunosamine sugar moiety is rather easily fragmented from the parent anthracycline as most experiments report the 397 m/z as the characteristic ion for doxorubicin (Figure 2-5). An m/z of 397 is also observed for standards of doxorubicinone (Figure 2-2, III); this is obtained by protonation and loss of a water molecule due to collision induced dissociation within the mass spectrometer. Doxorubicinol has an m/z of 546 due to the reduction of the carbonyl at carbon number 13 (Figure 2-1, Figure 2-2, II). And, 7-deoxydoxorubicinolone has an observed m/z of 399 (Figure 2-2, V). These mass fingerprints of the standard compounds allow for the identification of signal observed from more complex biological samples. This mass

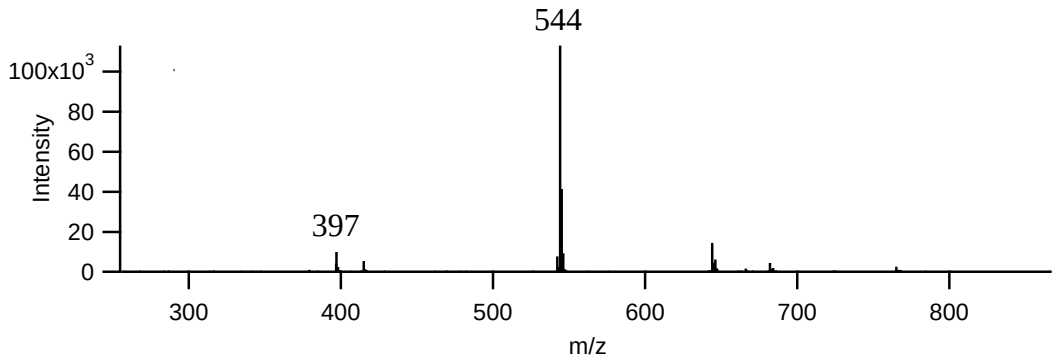

Figure 2-5. Mass spectrum of doxorubicin. An m/z of 544 is representative of the [M+H]+ ion. An m/z of 397 represents the fragmentation removing the daunosamine sugar moiety.

spectrometry data is used to identify chromatographic peaks of known and unknown compounds. Characteristic fragment ions (i.e. m/z 397 for doxorubicinone or m/z 399 for 7-deoxydoxorubicinone) can aid in linking observed unknown compounds as to originating from doxorubicin.

2.7. Analysis of Doxorubicin

Different separation based techniques use fluorescence detection (see section 2.5) to monitor doxorubicin and its fluorescent metabolic products. These techniques include, thin layer chromatography (TLC), high performance liquid chromatography (HPLC) and micellar electrokinetic chromatography (MEKC, a mode of capillary electrophoresis) [37, 57, 59].

Some early experiments used TLC as a separation technique and fluorescence and mass spectrometry as a detection scheme in order to examine the metabolic profiles of anthracyclines. In 1976, Takanashi, *et al*. reported the presence of a number of metabolic products of adriamycin (e.g. doxorubicin) in human urine. Those metabolites reported included: adriamycinol (Figure 2-2, II), adriamycinol aglycones (Figure 2-2, IV), deoxyadriamycinol aglycone (Figure 2-2, VI), as well as sulfates (Figure 2-2,

Table 2-3. Summary of separation and combined detection schemes used for the analysis of doxorubicin.

Separation	Detector	Reference
TLC	Fluorescence Spectroscopy	[10, 28]
HPLC	Fluorescence	[15, 44]
HPLC	Mass spectrometry	[57]
MEKC	Laser-induced fluorescence	[37, 43]

VIII) and glucuronides (Figure 2-2, IX). Identification of these metabolites was performed by comparison of fluorescence spectra and mass spectra with standard solutions of these compounds. A similar analysis was performed for doxorubicin [28].

More recently MEKC-LIF has been used to perform sensitive measurements on doxorubicin metabolism and localization within cells. Anderson, *et al.* report multiple peaks identified in separations of a single cell's contents and cell extracts that were treated with doxorubicin [37, 42, 43]. Due to the low limits of detection (i.e. zeptomole), up to 12 peaks attributed with the treatment of doxorubicin were detected. Unfortunately, MEKC-LIF alone is not well suited to identify these metabolites.

HPLC has been one of the most widely used tools in the analysis of doxorubicin [44, 57, 60-62]. HPLC with fluorescence, absorbance or mass spectrometry detection has been used extensively to monitor the metabolism of doxorubicin in blood plasma [45, 58, 60, 62] or urine [15, 28, 45] samples. Most studies focus on the analysis of doxorubicin and its two metabolites doxorubicinol (Figure 2-2, II) and doxorubicinone (Figure 2-2, III) [10, 15, 41, 57]. However, some previously reported metabolites[28]. (i.e. 7-deoxydoxorubicinolone, Figure 2-2, VI) have not been observed or studied in great detail in more recent studies.

In summary, HPLC, LIF, and MS, based on the merits of each analysis technique, was chosen in order to observe the metabolic profile of doxorubicin and its metabolites by collecting quantitative fluorescence data and structural MS data from liver tissue and explore the metabolism profile's change with age. The development and application of this instrumentation is described in Chapters 3 and 4.

Chapter 3

Tandem Laser-Induced Fluorescence and Mass Spectrometry Detection for High-Performance Liquid Chromatography Analysis of the In Vitro Metabolism of Doxorubicin

C. Eddy began assembly of the HPLC-LIF instrumentation. All data collection and analysis was performed by J. Katzenmeyer. Assistance with mass spectrometry instrumentation was provided by Dr. D. Reed and Dr. J. Dalluge (Directors of the Mass Spectrometry Facility, Department of Chemistry, University of Minnesota). Professor L. Thompson and her research group, primarily W. Torgerud, handled animal protocols and procedures.

3.1 Introduction

The combination of optical and mass detectors in tandem is a powerful resource to improve upon the characterization and analysis of complex samples and samples containing unknown compounds. Optical detection (e.g. UV-Vis absorption or fluorescence) allows for the quantitative data to be collected without the bias of ionization conditions. Mass spectrometry detection (MS) provides structural information of analytes that cannot be observed by spectroscopic methods. Surprisingly, very few reports describe combining UV absorption or laser-induced fluorescence (LIF) detectors with MS detectors. Crow, *et al.*, used high-performance liquid chromatography (HPLC) - UV-MS to characterize components of synthetic, toxic oil associated with toxic oil syndrome [63]. Akbay, *et al.*, reported the use of micellar electrokinetic chromatography with a tandem UV and MS detector to analyze a complex mixture of chiral beta-blockers [64]. Capillary electrophoresis (CE) with LIF-MS was used to obtain quantitative and structural data from an extract of dried leaves of *Psychotria viridis* [65]. CE-LIF-MS has also been used for the direct characterization of N-linked glycans in therapeutic antibodies [66]. Here we describe an HPLC-LIF-MS system and its use in the analysis of metabolites resulting from the biotransformation of doxorubicin in rat liver extracts.

Defining the pharmacological and toxicological profiles of xenobiotics requires both identifying and quantifying the products of their biotransformations. Mass spectrometry is an ideal method to obtain molecular structure data that assists in the identification of compounds, but more cumbersome when used for quantification purposes [51]. Using mass spectrometry for quantification would require the use of isotopically labeled standards or compounds with analogous molecular structures which

are not always available. In contrast, other detection schemes, such as fluorescence detection, are suitable for quantification of fluorescent xenobiotics (e.g. anthracyclines) [15, 42, 44] but inadequate for molecular characterization of unknown biotransformation products.

Doxorubicin is an anticancer anthracycline used to treat many cancer types, from solid tumors to leukemia. The metabolism of doxorubicin has been monitored in blood plasma, urine and cell cultures [15, 41, 43, 45, 57, 58, 62]. These analyses were performed with a separation technique such as thin-layer chromatography [41], CE [43] or HPLC [15, 45, 57, 58, 62] combined with varying detection schemes. For quantification, fluorescence detection is typically preferred [15, 41, 43, 45, 62] due to its selectivity and sensitivity. Unfortunately, the molecular structure of the detected metabolites cannot be determined with such detection scheme and their identity could only be speculated based on comigration with a few standards of known metabolites. Furthermore, the CE separation conditions are incompatible with mass spectrometry. Mass spectrometry is commonly used by monitoring characteristic mass peaks of doxorubicin and other anthracyclines through multiple reaction monitoring experiments [57, 58]. However, for quantification using mass spectrometry, an internal standard or isotopically labeled standard is typically used [44, 57, 67]. A tandem LIF-MS detector would eliminate the need of adding external standards to accomplish the desired quantification. Furthermore, the LIF sensitivity would help detect low abundance metabolites, even if they are not readily detected by MS.

In this chapter, we describe the development and use of a tandem LIF-MS detection scheme coupled with an HPLC system. This work demonstrated the

simultaneous separation (by HPLC), quantification (by LIF detection) and structural characterization (by MS) of doxorubicin and two of its metabolites, 7-deoxydoxorubicinolone and 7-deoxydoxorubicinone. MS data was not suitable for quantification, with relative standard deviations as high as 78% for peak area measurements in standard solutions. On the other hand, fluorescence measurements showed a relative standard deviation between repeat analyses of 7.5%. The HPLC-LIF-MS method described in this chapter could be easily extended to characterize and quantify other fluorescent compounds in increasingly complex samples of biomedical and environmental relevance occurring in vivo, *in vitro*, and in environmental systems. Furthermore, the tandem detection scheme would aid in validating HPLC separations of complex samples prior to the implementation of such separations in instruments with only LIF or MS detection.

3.2 Experimental

3.2.1 Materials

All materials were used as received. Water from a Millipore filter system (18 MΩ) was used for HPLC and buffer preparation. Acetonitrile, glucose-6-phosphate dehydrogenase type I and D-glucose-6-phosphate dipotassium salt hydrate were purchased from Sigma-Aldrich (St. Louis, MO). Formic acid, tris(hydroxymethyl)aminomethane (TRIS) and magnesium chloride were purchased from Fisher Scientific (Pittsburgh, PA). Sucrose was purchased from MP Biomedicals, Inc. (Illkirch, France). Monobasic potassium phosphate, perchloric acid, sodium hydroxide, hydrochloric acid, citric acid and potassium chloride were purchased from Mallinckrodt (Phillipsburgh, NJ). NADP was purchased from Roche Diagnostics, GmBH (Mannheim,

Germany). Doxorubicin was a generous gift from Meiji Seika Kaisha, LTD (Tokyo, Japan). Standards of doxorubicinol, doxorubicinone and 7-deoxydoxorubicinone were obtained from Qvantas, Inc. (Newark, DE).

3.1. Solutions

Tissue storage buffer consisted of sucrose (0.2 M), potassium phosphate (0.05 M) and potassium chloride (0.15 M) in water and adjusted to pH 7.4 with 0.1 M NaOH. Incubation buffer consisted of TRIS (0.05 M) and potassium chloride (0.15 M) in water. Glucose-6-phosphate dehydrogenase was reconstituted in citrate buffer (5 mM citric acid adjusted to pH 7.5 with 1 M sodium hydroxide) per the instructions accompanying the enzyme (Sigma-Aldrich G4134). The aqueous component of the HPLC mobile phase was Millipore filtered water with 0.1% Formic acid. The mobile phase was filtered with a 0.2 micron nylon filter (Gelman Sciences).

3.2.2 Tissue Procurement

10-months old Fischer 344 rats were purchased from the National Institute on Aging and housed in a research animal facility at the University of Minnesota. They were fed *ad libitum* standard laboratory rat chow and kept on a 12 hour light/dark cycle.

On the day of tissue harvesting, the rats were anesthetized with sodium pentobarbital (50 mg/kg body weight). Tissue was immediately removed and placed in the storage buffer on ice until homogenized. The rats were sacrificed after tissue harvesting. The animal protocol was approved by the University of Minnesota Institutional Animal Care and Use Committee.

3.2.3 *In Vitro* Metabolism

In vitro metabolism procedures were adapted from the literature [67, 68]. 1.6 g of rat liver tissue was homogenized in 3 mL of incubation buffer using 15 strokes of a Dounce homogenizer. The homogenizer was rinsed with 2 mL of incubation buffer and this solution was then added to the homogenate. Centrifugations were performed at 4° C. The tissue homogenate was centrifuged at 600×g for 10 minutes to remove tissue debris. The supernatant was subsequently removed and centrifuged at 10,000×g for 10 minutes creating a sediment consisting of heavy organelles (i.e. mitochondria) and a supernatant termed the post-mitochondrial fraction (PMF). This fraction contains microsomes common in many *in vitro* experiments as well as soluble cell components. The PMFs were used for the metabolism experiments. The biochemical reactions are expected to be caused by cytochrome P450 (CYP450) enzymes carbonyl reductase and NADPH - P450 reductase and NAD(P)H: quinone oxidoreductase; cofactors are added accordingly [29, 67, 68]. Magnesium chloride (5 mM), NADP (0.25 mM), glucose-6-phosphate (2.5 mM), and doxorubicin (50 µM) were added to final concentrations denoted by parentheses. The start of the reaction time was defined as the moment in which glucose-6-phosphate dehydrogenase (2.0 units) was added to the reaction mixture. The reaction mixture (final volume of 1.1 mL) was incubated at 37º C in a heated mixer (Eppendorf Thermomixer) and samples were removed at time intervals for analysis.

3.2.4 Extraction Procedure

An extraction procedure previously shown to result in 94.7 – 99.9% recovery of doxorubicin[62] was used to extract the compounds of interest from the biological matrix. The extraction solvent was prepared by mixing 14 µL of concentrated perchloric acid with 60 µL of HPLC mobile phase (67% water: 33% acetonitrile) in a 600 µL

microcentrifuge tube. At a selected reaction time, 40 µL of the reaction mixture were removed and pipetted into the extraction mixture. The tube was vortexed for 30 seconds and then centrifuged at 3000×g for 3 minutes. The supernatant was used directly for analysis.

3.2.5 HPLC-LIF-MS

An Agilent (Santa Clara, CA) 1100 capillary HPLC system was used in this analysis. A sample volume of 0.5 µL was injected into the HPLC apparatus and separated on a C18 column (0.3 x 150 mm, 3 µm particles, ACE11115003, Mac-Mod Analytical, Inc., Chadds Ford, PA). The mobile phase consisted of 67% water (0.1% formic acid) and 33% acetonitrile. The flow rate was set at 3.5 µL/min.

The HPLC column was connected to the electrospray ionization chamber of the mass spectrometer using 30 cm of 50 µm I.D. fused silica capillary (Figure 3-1). Teflon sleeves (Upchurch, F-242X) were used to adapt the outer diameter of the capillary to fit standard size

PEEK finger-tight fittings and reduce dead volume. For LIF detection, a 473 nm diode-pumped solid state laser (OnPoint Lasers, LTD, Eden Prairie, MN) was used for excitation. An approximately 5 mm section of the polyimide coating of the fused-silica capillary was burned off creating a detection window. A fluorescence flow-through cell (SpectrAlliance, Inc., St Louis, MO) equipped with fiber optics to deliver incident light and collect fluorescent light was used as an on-column detector. The collected fluorescence was filtered with a 580BP45 filter (Omega Optics) and monitored using a photomultiplier tube (Hamamatsu, biased at 800 V). Data from the photomultiplier tube

was digitized (10 Hz) using a National Instruments I/O board (PCI-6034E) run with a LabVIEW 5.1.1 (National Instruments, Austin, TX) program created in house. Using standards of doxorubicin, the alignment of the fluorescence detection window was properly placed in the detection zone of the flow-through device to achieve the maximum signal. A 10 µM solution of doxorubicin in methanol was passed through the capillary using a syringe adapter and a 100 µL syringe operated by a syringe pump at a flow rate of 3.5 µL/min. The capillary was secured with the nut on the flow-through device. The limit of detection was 2.0 µM or 1.0 x 10^{-12} moles of doxorubicin.

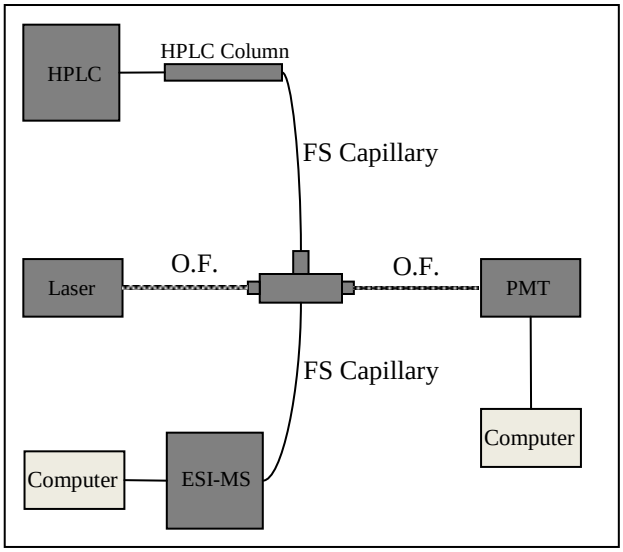

Figure 3-1 Diagram of HPLC-LIF-MS setup. The fused silica (FS) capillary (365 µm O.D., 50 µm I.D.) connecting the HPLC column and the ESI source was 30 cm long. The detection window was formed by burning an approximately 1 cm window in the polyimide coating. The interface between the fused-silica capillary and electrospray source was accomplished using a Teflon sleeve (Upchurch, F-242X) and a PEEK finger-tight fitting (Upchurch, F-300X). The ESI-MS instrument was a Bruker MicrOTOF$_Q$ mass spectrometer. The fluorescence cell (B) was obtained from SpectrAlliance and guides incident laser light (473nm) and fluorescent light via fiber optics (O.F., 1 m in length). Optical fibers, internal to the cell, guide incident light and fluorescent light at a 90º angle. PMT is a photomultiplier tube biased at 800 V; fluorescence was selected with a 580BP45 optical filter in front of the PMT; the data acquisition rate was 10 Hz.

Mass spectral data were collected using a Bruker MicrOTOF$_Q$ mass spectrometer (Bruker Daltonics Inc., Billerica, MA) capable of high accuracy MS and MS/MS data collection (10,000 to 15,000 mass resolution for m/z 350-800). Helium was used as the collision gas because doxorubicin was found to fragment extensively when using Argon. Positive

ions were detected. Calibration of the mass spectrometer was conducted using a dilute solution of sodium formate as the calibrant. The calibration solution was infused using a syringe pump at a flow rate of 3.5 µL per minute. Six m/z values (158.9641, 362.9263, 498.9012, 566.8886, 634.8760, and 770.8509) were used to conduct an enhanced quadratic calibration in the mass range of expected (i.e. doxorubicinol, doxorubicinone and 7-deoxydoxorubicinone) [10]. The parameters (funnel 1 and 2 RF, hexapole RF and collision RF) were adjusted to maximize the total ion current in the 300 to 850 m/z range. The limit of detection was ~ 10^{-12} moles of doxorubicin.

3.2.6 Separation and Detection Methods

In order to develop the separation and detection methods, standards of doxorubicin and two commonly reported metabolites (doxorubicinol and doxorubicinone) were used. These standards were prepared as stock solutions in methanol (1 mM) and diluted to obtain the desired concentrations. It was found that a C18 column was able to completely separate all components under isocratic conditions of 67% water and 33% acetonitrile. Due to the fact that an isocratic separation proved to be adequate, a gradient was not used for the separation. Using an isocratic method decreases the analysis time by eliminating an equilibration step of the HPLC instrument between separations. Using standard solutions and extracted tissue solutions there were no observed peaks by LIF or MS detection after a 20 minute separation time window. Therefore, carryover of peaks between samples was not of concern.

3.2.7 Data Analysis

MS detection of an eluting peak lagged 29±1 seconds relative to fluorescence detection. This time difference was used to associate MS and LIF signals. MS data were

analyzed using DataAnalysis 4.0 supplied by Bruker Daltonics. Fluorescence data were analyzed using in house developed Igor Pro procedures (WaveMetrics, Inc., Portland, OR).

The fluorescence quantum yields of doxorubicinol and 7-deoxydoxorubicinone relative to doxorubicin were determined by comparing total fluorescence intensities of equimolar (10 μM) solutions in HPLC mobile phase. The total fluorescence intensity was measured with a spectrofluorometer (Jasco FP-6200, 465 nm excitation) over the 557-602 nm range, which matches the transmission range of the 580BP45 optical filter in the LIF detection apparatus, The relative quantum yield of 7-deoxydoxorubicinone to doxorubicin was 1.0±0.1 (n=3). The relative quantum yield of doxorubicinol to doxorubicin was 1.7±0.1 (n=3). Since doxorubicin and the aglycone 7-deoxydoxorubicinone (i.e. doxorubicin without the daunosamine moiety) have the same quantum yield, we assumed that doxorubicinol and 7-deoxydoxorubicinolone (i.e. doxorubicinol without the daunosamine moiety) have also a similar fluorescence quantum yield.

The transformation of doxorubicin into metabolites was expressed in terms mole fractions using the expression

$$n_i = \frac{C_i}{\sum C_i} \tag{3-1}$$

in which n_i is the mole fraction corresponding to compound (i) (i.e. doxorubicin, doxorubicinone, 7-deoxydoxorubicinone, or 7-deoxydoxorubicinolone), and C_i is the concentration of compound (i). Each C_i was determined using the expression

$$C_i = F\frac{A_i}{\Phi_F} \qquad (3\text{-}2)$$

where F is LIF detector response factor relating doxorubicin concentration to total fluorescence peak area in the sample at t=0 minutes of incubation determined for each set of data, ϕ_F is the fluorescence quantum yield, and A_i is the area of the peak. Both doxorubicin and doxorubicinone peaks must be included in the F factor because they are detected at t=0 and represent 50 µM doxorubicin used at the onset of the reaction. It is worth noticing that for each sample taken at different reaction times, it is expected that $\sum Ci \sim 50$ µM. In practice, this sum varies from 35 µM to 54 µM.

Chemical compositions were calculated from the acquired MS data using the Bruker Data Analysis software. The MicrOTOF$_Q$ routinely collects spectra with 10,000 to 11,000 mass resolution and ~0.2 mDa precision, and tolerances ~ 10 ppm, which is adequate to generate an initial list of possible chemical compositions. Unfortunately, this list still has many possible chemical formulas for each observed mass. For example, a compound with m/z of 400 and a 10 ppm mass tolerance would be expected to generate 50-60 elemental compositions containing C, H, N, O and S [56]. In this study, the calculated elemental compositions in combination with prior knowledge of the parent drug and likely biochemical transformations, allowed the selection of the most likely candidate molecules. The two restrictions used were: (i) the maximum number of nitrogen atoms in the chemical formula was set to two, and (ii) the mass tolerance was 20 ppm. Using these restrictions the maximum number of chemical formulas for each compound detected was five. Among these formulas, the selection of the best match was strongly dependent on its sigma value, which is an index of the deviations of observed

from the predicted masses and intensities of monoisotopic peaks corresponding to given chemical formula. When using standard compounds, the formula with the lowest sigma value was the correct chemical composition; this was not the case for the metabolism samples, but prior knowledge on doxorubicin metabolism, comparison of retention times with standards, and very low sigma values increased the confidence of the compounds' identifications.

3.3 Results and Discussion

3.3.1 Recovery After Extraction

Initially, we attempted to recover doxorubicin metabolites by solid-phase extraction (SPE) using a C18 SPE cartridge (Waters) [57]. While extraction of standards from buffer solutions recovered 99% of doxorubicin and the standard metabolites, the approach failed to recover reproducibly the same standards from a biological matrix (i.e. homogenized liver tissue). A second extraction method based on previous work that uses perchloric acid treatment provided the best reproducibility and recovery [62]. This procedure recovered 98±1% of doxorubicin, doxorubicinol and doxorubicinone standards from liver tissue homogenate.

3.3.2 Validation of Tandem LIF-MS Detection System

LIF was adequate to detect chromatographically separated standards of doxorubicin, doxorubicinol, and doxorubicinone. The linear range for peak area versus concentration was between 2 µM and 50 µM doxorubicin (the range tested). The separation efficiency was ~ 17,000 theoretical plates for doxorubicin (Table 3-).

MS Detection was delayed by 29±1 seconds compared to the LIF detection due to the extra distance of travel to the ESI source. The separation resolution and the number of theoretical plates were reduced in MS relative to LIF detection (Table 3-). Diffusion, which explains only 0.0007% of MS peak broadening, does not explain the degradation of the separation occurring between the LIF and MS detectors (Appendix A) [69]. Peak tailing, due to adsorption of doxorubicin and the metabolites to the silica surface is similar in both LIF and MS peaks [70]. Thus, adsorption cannot explain the lower separation performance at the MS detector. The most likely contributor to peak broadening is the ESI interface to the mass spectrometer. The inner diameter of the sprayer needle is 90-100 µm which is larger than the 50 µm capillary connecting to the MS ionization chamber. This can cause significant peak broadening as the analytes reach this connection point [70]. Although it would be desirable to re-design the interface to the mass spectrometer to maintain a good separation performance, a more relevant issue was that the peak area response from the MS detector was erratic.

For example, the MS chromatogram peak area for doxorubicin with repeated injections of standards was found to be up to 78% relative standard deviation. Therefore, LIF data was used for quantification purposes.

Table 3-1. Resolution and separation efficiencies for both detectors. N and t_1 are the number of theoretical plates and retention time, respectively, of Peak 1, doxorubicin. $R_{1,2}$ is the resolution between peaks 1 and 2. See Figure 3-2 for peak assignments.

Detector	N	$R_{1,2}$	t_1 (s)
LIF	17000±2000	6.1±1.2	360±30
MS	4100±300	3.1±0.5	390±30

3.3.3 Separation of Doxorubicin and Its Metabolites

The tandem LIF and MS detector was adequate to monitor biotransformation of doxorubicin in the PMF from a rat liver. Figure 3-2 shows a separation of the PMF of the liver tissue incubated with doxorubicin for 10 minutes then extracted and analyzed by HPLC-LIF-MS. The LIF chromatogram (lower trace) and the corresponding MS chromatogram (upper trace) are comprised of doxorubicin (Peak 1) and possible metabolites (Peaks 2, 3 and 4). For LIF detection, an efficiency of 15250 theoretical plates is achieved for doxorubicin, 7200 theoretical plates for Peak 2, and 8600 for Peak 4. Resolutions for each peak are greater than 1.0 except for Peaks 2 and 3 (Resolution ~ 0.8). However, Peaks 2 and 3 can be distinguished from each other by examining the mass spectra. Furthermore, while all observed signals detected by LIF have corresponding MS signals, there are components that are only present in the MS chromatogram. These components correspond to biological matrix because they are also present in the absence of doxorubicin treatments (See Figure A-1, Appendix A). Identifying these components was outside the scope of this work.

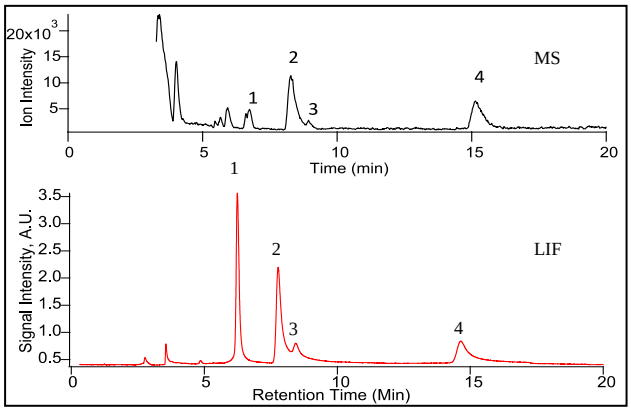

Figure 3-2. Mass and LIF chromatograms of a liver PMF treated with doxorubicin. The PMF was treated with 50µM doxorubicin, extracted after 10 minutes, and processed as described in the experimental. A volume of 0.5 µL was injected into the HPLC system. Separation was conducted in a 150×0.3 mm C18 column (ACE11115003, Mac-Mod) under isocratic conditions (67% water, 0.1% formic acid: 33% acetonitrile). The detection conditions are described in Figure 3-1.

3.3.4 Analysis of Mass Spectrometry Data

The accurate mass determination approach was used to determine the identities of doxorubicin (Figure 3-3A) and compounds resulting from the doxorubicin treatment of the PMF fractions (Figure 3-3B-D). The latter figures show that the predominant m/z values for compounds derived from doxorubicin are 401.1182, 397.0873 and 399.1022. Table 3-2 is a summary of identities, calculated masses, observed masses and errors. Doxorubicin (Peak 1 in Figure 3-2, Figure 3-3A, Figure 3-4) has an observed characteristic m/z value of 544.1824 (theoretical m/z 544.1813 for $(M+H)^+$) with a minor fragment observed at 397.0873 m/z (theoretical m/z 397.0923). From the mass spectra in Figure 3-3D, Peak 4 in Figure 3-2 was identified as 7-deoxydoxorubicinone (Figure 3-4). This aglycone metabolite has a molecular mass of 398.3628 Da. The protonated ion form has an m/z value of 399.1079 Da which is within a 10.7 ppm mass deviation of 399.1022 m/z, the observed mass. Furthermore, the retention times of the observed compound (Peak 4, Figure 3-2) and 7-deoxydoxorubicinone standard were both 15.3 minutes.

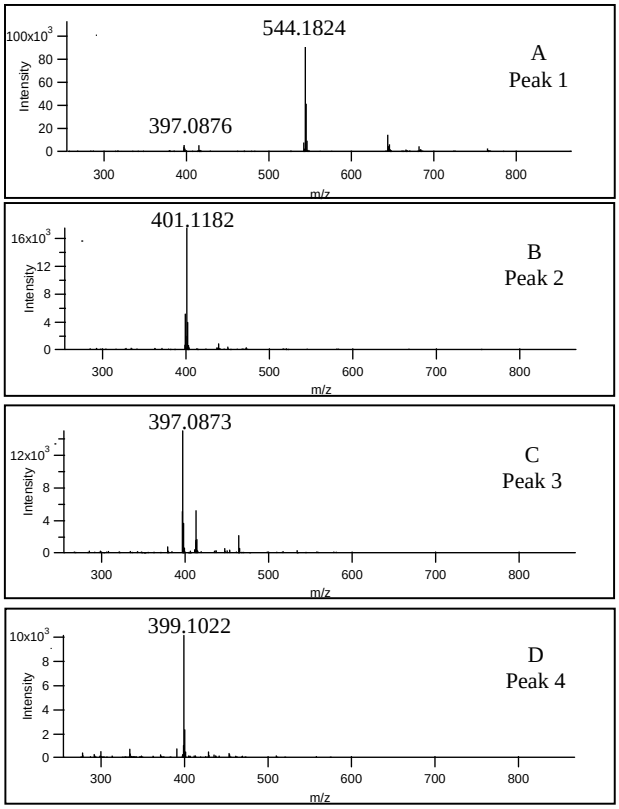

Figure 3-3. Mass spectra of compounds detected compounds. See Figure 3-2. The mass spectra were averaged across chromatographic peaks.

Table 3-2. Identities of the peaks observed in MS chromatograms. See Figure 3-2 for peak assignments.

Peak	Identity	Measured Mass (m/z)	Calculated Mass (m/z)	Mean Error (ppm)	Retention Time (min)
1	Doxorubicin	544.1824	544.1813	1.9	6.2
2	7-deoxydoxorubicinolone	401.1182	401.1194	6.9	8.1
3	Doxorubicinone	397.0873	397.0923	6.8	8.7
4	7-deoxydoxorubicinone	399.1022	399.1079	10.7	15.3

Similarly, Peak 2 in Figure 3-2 was identified as 7-deoxydoxorubicinolone (Figure 3-4). The m/z value of 401.1182 (Figure 3-3B) is within 6.8 ppm error of the calculated mass of 7-deoxydoxorubicinolone, 401.1194 Da. The accurate mass measurements were particularly useful in ruling out a second match for Peak 2. This false match is the demethylated form of doxorubicinone that has a calculated m/z of 401.0867 for the $(M+H)^+$ ion. The mass of the demethylated metabolite, however, is a 78.5 ppm mass deviation from the observed value (401.7782) and is therefore a much less likely candidate than 7-deoxydoxorubicinolone.

Peak 3 in Figure 3-2 was identified as doxorubicinone (Figure 3-4). While the molecular mass of doxorubicinone is 414.3622 Da, the observed value is 397.0873 m/z value (Figure 3-3C), which appears to be caused by protonation and loss of one water molecule resulting from collision induced dissociation. This ion is the same as a fragment observed in the doxorubicin mass spectrum (c.f. Figure 3-3A). However, doxorubicinone is clearly identified because the retention time of Peak 3 in Figure 3-2 (i.e. 8.7 minutes) matches that of doxorubicinone standards (i.e. 8.6 minutes).

Doxorubicinone is an aglycone metabolite of doxorubicin that results from oxidative cleavage of the daunosamine sugar [71] but also form as a result of acid catalyzed cleavage of the daunosamine sugar during the sample preparation. In fact, a

control using only a doxorubicin standard in incubation buffer followed by perchloric acid extraction also resulted in doxorubicinone detection after 20 minutes of exposure to the acid (data not shown). Therefore, it is not possible to determine the relative contributions of metabolic or acid catalyzed reactions to doxorubicinone formation.

The m/z value for doxorubicinol (one of the most commonly reported metabolites) [71-74], 546 m/z, was not observed in any experiments conducted here. Doxorubicinol standard is easily detectable in both LIF and MS when extracted from biological material and analyzed using this procedure (See Figure A-2, Appendix A), which rules out an inadequate extraction and detection scheme. While it is possible that carbonyl reductase, the enzyme responsible for the conversion of doxorubicin to doxorubicinol, has low activity in the PMF of rat liver, a more likely explanation is that any doxorubicinol that formed is rapidly transformed into doxorubicinol by carbonyl reductase [29] and then quickly transformed into 7-deoxydoxorubicinolone (Figure 3-4), which is in agreement with the scheme proposed by Takanashi, et al [75]. Based on this argument, both doxorubicin and doxorubicinol are converted further by NADPH – cytochrome P450 reductase and NAD(P)H: quinone oxidoreductase producing the aglycone metabolites 7-deoxydoxorubicinone and 7-deoxydoxorubicinolone (Figure 3-4) [29].

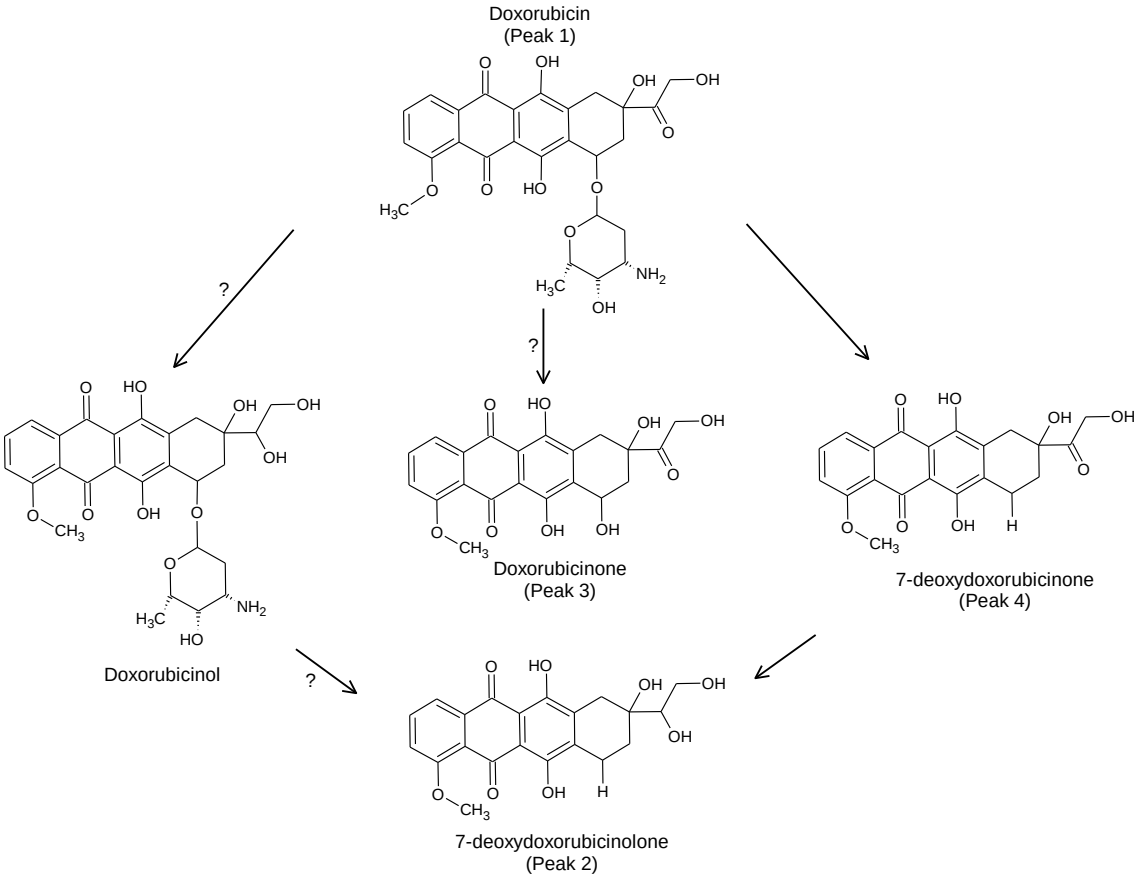

Figure 3-4. Proposed doxorubicin metabolism by the rat liver PMF. Compound detection (Figure 3-2) and identification (Figure 3-3) indicate that 7-deoxydoxorubicinone and 7-deoxydoxorubicinolone are present. Doxorubicinol was not detected in this study. Doxorubicinone forming due to acid hydrolysis or metabolic transformation is indistinguishable in this study. Question marks indicate metabolic pathway that cannot be elucidated with the current information.

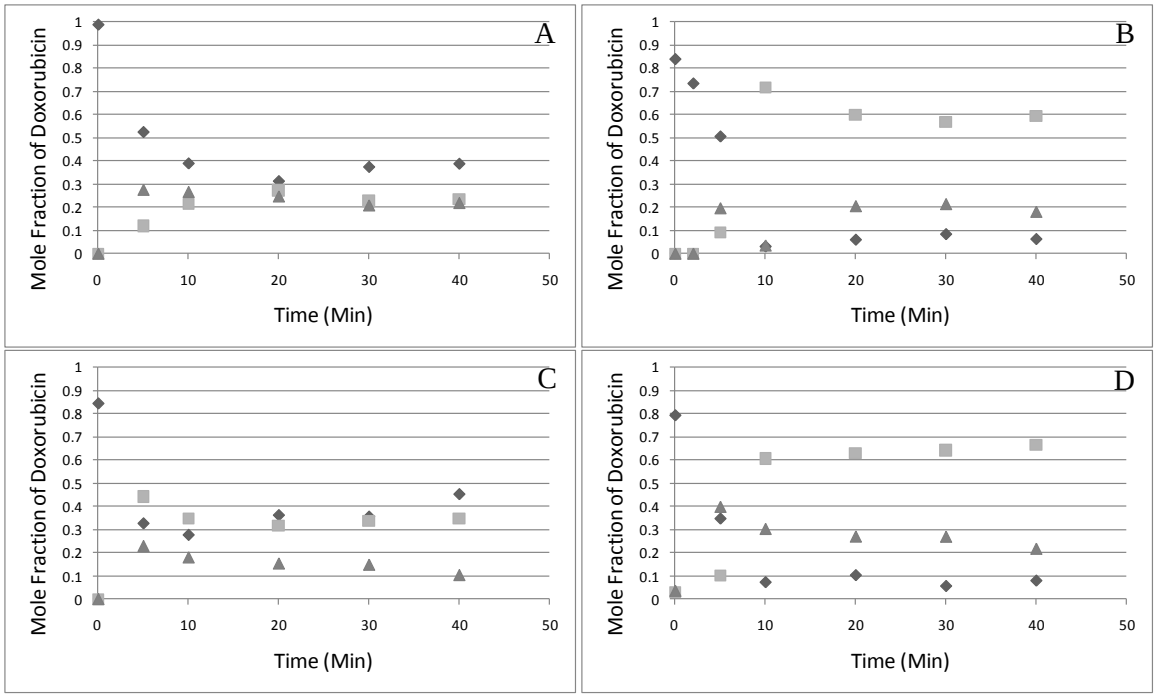

Figure 3-5. Doxorubicin biotransformation dynamics in a rat liver PMF. Mole fractions were calculated using Equation 3-1. Diamonds represent doxorubicin (peak 1); squares represent 7-deoxydoxorubicinolone (peak 2); and triangles represent 7-deoxydoxorubicinone (peak 4). Parts A through D correspond to different animals. Other conditions are given in Figure 3-2.

The lack of formation of doxorubicinol in this report may be reconciled with the observed formation of this metabolite in other studies, by considering the enzymatic composition of the *in vitro* systems under investigation. In other studies, the *in vitro* systems are cytosolic fractions without microsomes and the enzymes (cytochrome P450s) responsible for cleaving the daunosamine sugar of doxorubicin [74]. In our *in vitro* system, the PMF includes microsomes, thereby providing a different metabolic profile for rat liver.

3.3.5 Biotransformation Dynamics Monitored by LIF

The quantitative power of the LIF detector was used to monitor the dynamics of the *in vitro* metabolism of doxorubicin in four different animals (Figures 3-5 A-D). Doxorubicin and its metabolites were expressed as mole fractions (c.f. Equations 3-1 and 3-2), which avoided complications caused by differences in the fluorescence quantum yields of the various compounds. As observed in Figure 3-5, while doxorubicin (diamonds) was consumed, 7-deoxydoxorubicinolone (Peak 2, squares) and 7-deoxydoxorubicinone (Peak 4, triangles) increased. After ~10 minutes, little or no change was noticed. Based on Equation 3-1, metabolite concentrations (at 30 minutes) were 29 µM 7-deoxydoxorubicinolone and 11 µM 7-deoxydoxorubicinone. It is important to note that MS detection was not suitable to monitor the dynamics of the *in vitro* metabolism (Figure A-3, Appendix A).

In two cases (i.e., Figure 3-5A and C), an increase in doxorubicin content is observed after reaching a plateau. Both biosynthesis of doxorubicin and variations in detector response are unlikely explanations. In expressing the concentrations of each compound as a mole fraction of doxorubicin, the sum of the concentrations of the four

observed compounds is effectively normalized to the initial doxorubicin concentration (50 µM). Therefore, any increase in signal due to a variation in detector response would be eliminated since the sum of all concentrations is taken to be 50 µM in all samples. On the other hand, the difficulty in controlling the length of the extraction procedure because each sample is prepared separately may result in variable acid hydrolysis of doxorubicin to form doxorubicinone. In order to investigate this possibility, we replotted Figure 3-5C combining the mole fractions of doxorubicin and doxorubicinone (Figure A-4, Appendix A). The apparent increase in doxorubicin disappears.

Not surprisingly, the PMF of each animal exhibited unique biotransformation dynamics, yet consistently forms 7-deoxydoxorubicinolone (squares, Figure 3-5) and 7-deoxydoxorubicinone (triangles, Figure 3-5). Clearly, these temporal biotransformation profiles are proof-of-principle of a method that could be easily extended to other fluorescent xenobiotics of biomedical or environmental relevance, which are described in the Section 5.2, Future Work.

3.4 Concluding Remarks

The HPLC-LIF-MS setup described here was adequate to collect simultaneously both structural and quantitative data needed to identify and quantify *in vitro* metabolism products of doxorubicin from rat liver. The high resolution and high mass accuracy of the MicrOTOF$_Q$ narrowed down the number of possible structures of metabolites and revealed 7-deoxydoxorubicinolone and 7-deoxydoxorubicinone are formed, while doxorubicinol, considered a major metabolite in plasma from patients treated with doxorubicin [74, 76] is not detectable. The LIF detector made it possible to estimate concentrations of doxorubicin and its metabolites over the course of an *in vitro* metabolic

study. Future applications of HPLC-LIF-MS systems may include the analysis subcellular factions and intracellular localization of doxorubicin metabolites in cytotoxicity studies [77-79] *in vivo* metabolism of other fluorescent xenobiotics, biotransformations in different tissue types [71, 80] or metabolic alterations associated with disease and human aging [22]. Lastly, the tandem detection scheme described here may have wide applicability in the analysis of fluorescent compounds because it would aid in validating HPLC separations of complex samples prior to the implementation of such separations in instruments with only LIF detection. That is, once the identities of the compounds have been established and interferences have been ruled out, the methods could be directly transferred to instruments with only spectroscopic detection [81].

Chapter 4

An HPLC-LIF-MS Method to Evaluate the Effect of Aging on the Metabolism of Doxorubicin in Fischer 344 Liver Post-Mitochondrial Fractions

This work is unpublished at the time of submission of this thesis.

All HPLC-LIF-MS data collection and analysis were performed by J. Katzenmeyer. MEKC-LIF work was done by Y. Wang and is included here with permission. Assistance with mass spectrometry instrumentation was provided by Dr. D. Reed and Dr. J. Dalluge (Directors of the Mass Spectrometry Facility, Department of Chemistry, University of Minnesota). Professor L. Thompson and her research group, primarily W. Torgerud, handled animal protocols and procedures.

4.1. Introduction

Upon entering our bodies, either through diet, air, drinking water, or drug administration, xenobiotic compounds may experience a multitude of biochemical processes. Many processes are intended as detoxication to make the xenobiotic less toxic, more polar and more readily excreted [2]. However, these biochemical processes may also change the activity of drugs or other seemingly inert compounds that then may have adverse effects on the human body [2]. This is particularly a critical issue among elders who usually take several medications [19] and whose ability to metabolize such medications may be dramatically different from that of a younger individual.

The effect that the age of an organism has on the metabolism of a xenobiotic compound or drug is a contested and difficult factor to measure [22]. Some studies measured the decrease in metabolism in elderly patients. For example, a 30% decrease in both *in vivo* and *in vitro* metabolism of antipyrine by cytochrome P450 enzymes was reported after age 70 [5]. Even more complicated studies focused on adverse interactions of medications resulting from the effect of age on the metabolism and clearance of drugs in the elderly [7]. These studies highlight the need for better analytical strategies to assess age-related metabolic changes.

In order to evaluate changes in metabolizing ability with age, many animal models have been explored because they age faster than human subjects. Lee *et al*. found that in Brown Norway rats the expressions of a number of xenobiotic metabolizing enzymes were affected by age [4]. In a majority of cases, the gene expression for CYP450s (enzymes prominent in metabolism pathways) was decreased, on average, by 2 to 3 times with age. A second study using male Wistar rats as models to examine changes

in cytochrome P450 enzymes with age reports an age-related decrease in metabolizing enzyme's activity [6]. However, the intracellular mechanisms causing the decrease in activity are yet to be discerned.

A decrease in metabolism with age leads to the possibility of an increase in adverse effects on an organism with age, even mortality. A study using young and old rats *in vivo* and *in* vitro found that doxorubicin concentrations in the serum and organs were 1.5 to 2 times higher in Male Crl:CD (SD) BR rats of the old age group [72]. The mortality rates of these rats over the course of the study (270 days of observation) were also altered with age. A dose of 2.5 mg/kg of doxorubicin was not lethal rats in the young age group (6 to 8 weeks old). However, this dose was lethal to the two animals observed in the old age group (24 months old).

Doxorubicin has been studied previously using both fluorescence and mass spectrometry. The native fluorescence of doxorubicin and its metabolites was used to monitor the concentrations of the parent drug as well as metabolic products [73, 82]. Mass spectrometry was used to identify metabolites of doxorubicin such as doxorubicinol, doxorubicinone, 7-deoxydoxorubicinone and 7-deoxydoxorubicinolone, the latter three exhibiting a loss of the sugar moiety (Figure 4-1) [83]. Chapter 3 describes the use of high-performance liquid chromatography (HPLC) with tandem laser-induced fluorescence (LIF) and mass spectrometry (MS) detection to collect both quantitative fluorescence and structural MS data [84]. The use of the tandem LIF-MS detectors proved to be a

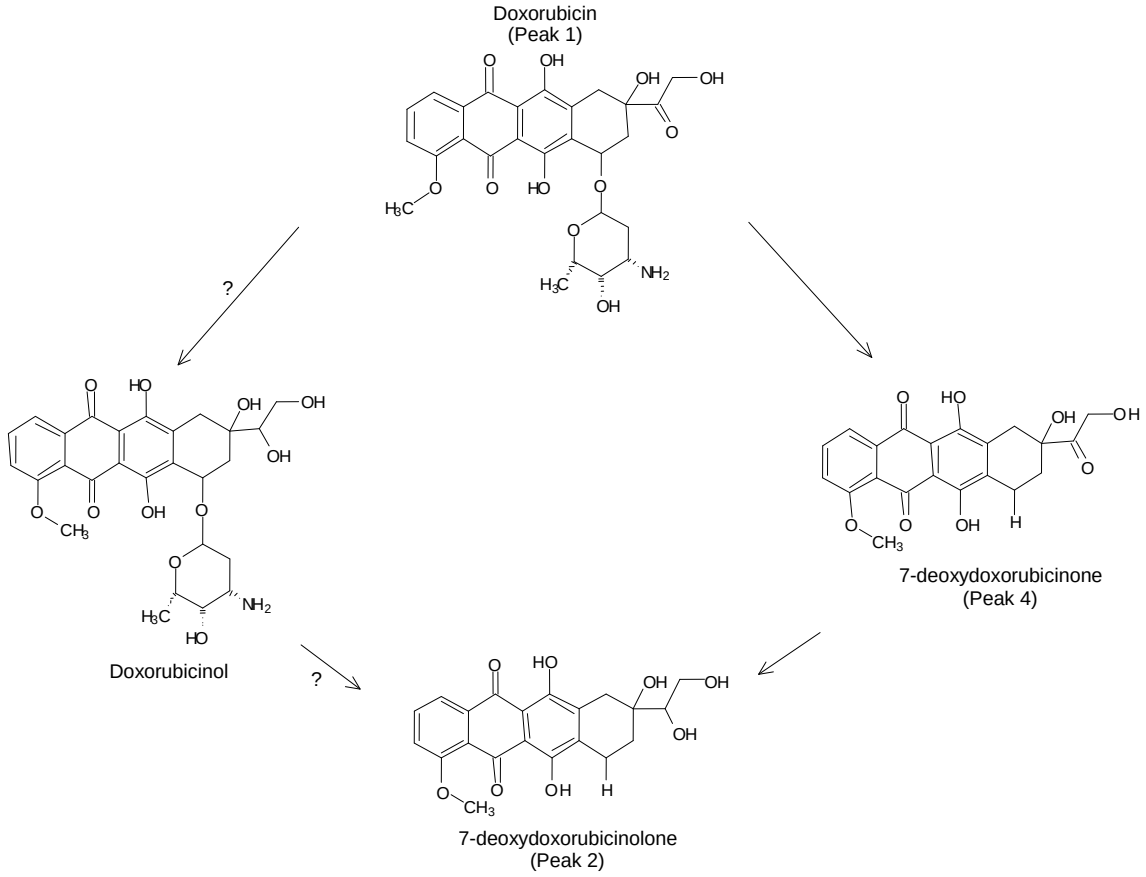

Figure 4-1. Suggested pathways of doxorubicin biotransformation.

powerful tool in identifying and quantifying metabolic products of doxorubicin from liver tissue *in vitro*.

This chapter describes the work that evaluated the suitability of HPLC-LIF-MS to detect age-related differences in metabolism of doxorubicin. First it showed that doxorubicin metabolism is more active in the liver than in the heart of young adult Fischer 344 rats (10 months old, 100% survival rate). Second it compared the doxorubicin metabolism in the young adult and old Fischer 344 rats (26 months old, ~25% survival rate). Both 7-deoxydoxorubicinolone and 7-deoxydoxorubicinone (Figure 4-1) were common to both age groups. However, the rates of biotransformations decreased in the 26 months-old age group. The timeframe required to reach a steady state level was longer and more variable in the 26 months-old age group as well. The steady state concentrations were not observed to vary between the age groups. The technology presented here could be easily applied to *in vitro* and *in vivo* age-related metabolic studies of natively fluorescent drugs and xenobiotics which are described in Chapter 5.2, Future Work.

4.2. Methods

4.2.1. Materials

All materials were used as received. Water from a Millipore filter system (18 MΩ) was used for HPLC and buffer preparation. Acetonitrile, nicotinamide adenine dinucleotide phosphate ($NADP^+$), glucose-6-phosphate dehydrogenase type I and D-glucose-6-phosphate dipotassium salt hydrate, and dimethylsulfoxide (DMSO) were purchased from Sigma-Aldrich (St. Louis, MO). Formic acid, Tris and magnesium

chloride were purchased from Fisher Scientific (Pittsburgh, PA). Sucrose and dicumarol were purchased from MP Biomedicals, Inc. (Illkirch, France). Monobasic potassium phosphate, perchloric acid, sodium hydroxide, hydrochloric acid, citric acid and potassium chloride were purchased from Mallinckrodt (Phillipsburgh, NJ). $NADP^+$ was purchased from Roche Diagnostics, GmBH (Mannheim, Germany). Doxorubicin was a generous gift from Meiji Seika Kaisha, LTD (Tokyo, Japan). Standards of doxorubicinol, doxorubicinone and 7-deoxydoxorubicinone were obtained from Qvantas, Inc. (Newark, DE).

4.2.2. Solutions

Tissue storage buffer contained sucrose (0.2 M), potassium phosphate (0.05 M) and potassium chloride (0.15 M) in water and was adjusted to pH 7.4 with 0.1 M NaOH. Incubation buffer consisted of Tris (0.05 M) and potassium chloride (0.15 M) in water. Glucose-6-phosphate dehydrogenase was reconstituted in citrate buffer (5 mM citric acid adjusted to pH 7.5 with 1 M sodium hydroxide) per the instructions accompanying the enzyme (Sigma-Aldrich G4134). The aqueous component of the HPLC mobile phase was Millipore-filtered water with 0.1% formic acid. The mobile phase was filtered subsequent to the addition of formic acid using a 0.2 micron nylon filter (Gelman Sciences). A stock solution of dicumarol was prepared in DMSO (10 μM).

4.2.3. Tissue Procurement

10-month old and 26-month old male Fisher 344 rats were purchased from the National Institute on Aging and housed in a research animal facility at the University of Minnesota. They were fed *ad libitum* standard laboratory rat chow and kept on a 12 hour light/dark cycle.

Liver and heart tissue was collected from the rats. On the day of tissue harvesting, the rats were anesthetized with sodium pentobarbital (50 mg/kg body weight). Tissue was immediately removed and placed in the storage buffer on ice until homogenized. The rats were sacrificed after tissue harvesting. Animals were sacrificed on separate days to allow the complete analysis of the sample on the day of sacrifice. The animal protocol was approved by the University of Minnesota Institutional Animal Care and Use Committee.

4.2.4. *In Vitro* Metabolism

In vitro metabolism procedures were adapted from the literature [85, 86]. Rat liver tissue (1.6 g) was homogenized in 3 mL of incubation buffer using 15 strokes of a Dounce homogenizer. The homogenizer was rinsed with 2 mL of incubation buffer and this solution was then added to the homogenate. Centrifugations were performed at 4° C. The tissue homogenate was centrifuged at 600×g for 10 minutes to remove tissue debris. The supernatant was subsequently removed and centrifuged at 10,000×g for 10 minutes creating a pellet consisting of heavy organelles (e.g. mitochondria) and a supernatant termed the post-mitochondrial fraction (PMF). This fraction contains microsomes and soluble cytosolic components common in many *in vitro* experiments. The PMFs were used for the metabolism experiments.

The heart (1.1 g) was cut into small pieces (~2 mm in size) and placed in 3 mL of incubation buffer. The blade homogenizer (TissueTearor 985-370, Biospec Products, Inc.) was used to homogenize the heart tissue in 5 s pulses until no pieces larger than 1 mm remained. An additional 2 mL of incubation buffer was added to the mixture. This homogenate was used directly in the *in vitro* experiments.

In vitro metabolism was carried out by adding appropriate cofactors and doxorubicin, at final concentrations indicated in parentheses, to the PMF. These are: Magnesium chloride (5 mM), $NADP^+$ (0.25 mM), glucose-6-phosphate (2.5 mM), and doxorubicin (50 μM). The start of the reaction time was defined as the moment in which glucose-6-phosphate dehydrogenase (2.0 units) was added to the reaction mixture. The reaction mixture (final volume of 1.1 mL) was incubated at 37º C in a heated mixer (Eppendorf Thermomixer). In addition, experiments using dicumarol (1 μM) as an inhibitor of NADPH-P450 reductase were performed in order to induce the formation of doxorubicinol [29]. The dicumarol solution was added immediately prior to the addition of the glucose-6-phosphate dehydrogenase.

Samples analyzed by MEKC-LIF were prepared in the following manner: Doxorubicin (10 μM) and cofactors (1 mM NADPH and 5 mM $MgCl_2$) were added into post-mitochondrial fractions (PMF) of young and old rat liver for *in vitro* metabolism. The mixtures were incubated at 37 ºC with mild vortexing. Samples were taken out after 15 min, 30 min, 1 h and 2 h incubation. The reaction was stopped by freezing the sample in dry ice. The samples were kept at -80 ºC until analysis.

4.2.5. Sampling Procedure

The sampling procedure has been previously described [84, 87]. Briefly, the extraction solvent was prepared by mixing 14 μL of concentrated perchloric acid with 60 μL of HPLC mobile phase (67% water: 33% acetonitrile) in a 600 μL microcentrifuge tube. At a given reaction time, 40 μL of the reaction mixture were removed and pipetted into the extraction mixture. The tube was vortexed for 30 seconds and then centrifuged at 3000×g for 3 minutes. The supernatant was used directly for analysis.

Samples from liver PMF incubated with doxorubicin were taken at 0, 10, 20, 30, and 40 minutes after initiating the reaction and extracted as indicated above. For heart tissue incubated with doxorubicin, the samples were taken at 0, 20, 40, 60 and 120 minutes after the onset of the reaction.

4.2.6. HPLC-LIF-MS

A diagram of the instrument setup used in these experiments is presented in Figure 4-2A. Briefly, an Agilent (Santa Clara, CA) 1100 capillary HPLC system instrument was employed for the separation. For detection of doxorubicin and metabolites, an LIF detector for quantitation and a MS detector for structural identity were used in tandem and have been described previously [84]. A sample volume of 0.5 µL was injected into the HPLC apparatus and separated on a reverse-phase, C18 column (ACE11115003, Mac-Mod Analytical). The separation was carried out isocratically with a mobile phase consisting of 67% water (0.1% formic acid) and 33% acetonitrile. The flow rate was set at 3.5 µL/min. The HPLC column was connected to the electrospray ionization chamber of the mass spectrometer with a fused-silica capillary. An approximately 5 mm section of the polyimide coating of the fused-silica capillary was burned off creating a detection window.

LIF detection was accomplished on-column at the detection window using a fluorescence flow-through cell (SpectrAlliance, Inc.) equipped with fiber optics to deliver incident light (473 nm, diode-pumped, solid-state laser) and collect fluorescent light

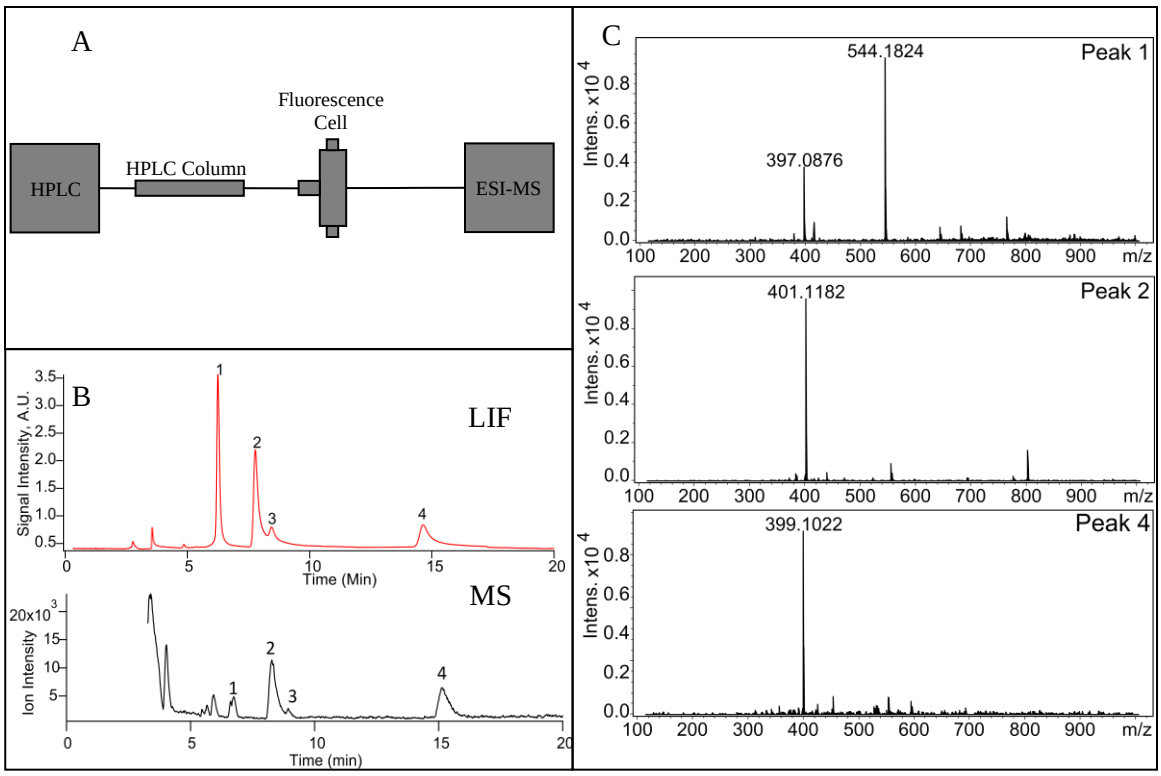

Figure 4-2. HPLC-LIF-MS of doxorubicin metabolic products. (A) Schematic diagram of the instrument setup. (B) LIF (top) and base peak MS (bottom) chromatograms. (C) Mass spectra of the peaks in (B). Peak 1 is doxorubicin; peak 2 is 7-deoxydoxorubicinolone; peak 3 is doxorubicinone; and peak 4 is 7-deoxydoxorubicinone.

(filtered with a 580BP45 filter and monitored using a photomultiplier tube). Data from the photomultiplier tube was collected using a LabVIEW 5.1.1 program created in house.

Mass spectral data were collected using a Bruker MicrOTOF$_Q$ mass spectrometer (Bruker Daltonics Inc., Billerica, MA) capable of high mass precision (0.2 mDa) and high mass resolution (10,000 to 13,000 mass resolution for m/z 350-800) for MS and MS/MS data collection. This high precision mass data allows the calculation of chemical compositions from the observed masses. The assignment of chemical compositions can be routinely carried out with differences between observed and theoretical masses within 10 ppm mass deviation. Helium was used as the collision gas because doxorubicin was found to fragment extensively when using Argon. Positive ions were detected. Metabolites of doxorubicin are expected to have an m/z between 300 m/z and 850 m/z. These include the metabolites previously reported by other groups (i.e. doxorubicinol, doxorubicinone and 7-deoxydoxorubicinone) [71].

4.2.7. Micellar Electrokinetic Chromatography With Laser-Induced Fluorescence Detection (MEKC-LIF)

In order to confirm age-related changes in metabolism, experiments using independent methods of separation were performed. MEKC is a mode of capillary electrophoresis (CE) that employs micelles (e.g. dodecylsulfate micelles) as a pseudostationary phase for separation of neutral molecules. When combined with LIF detection, this technique offers exquisite limits of detection [37]. In this report, MEKC-LIF was used to compare the trends of formation of the main metabolites and also detect compounds that are undetected and unidentified by HPLC-LIF-MS. Before analysis, samples were diluted with separation buffer (50 mM borate, 50 mM SDS and 20 mM γ-

cyclodextrin, pH = 9.3) (BS50-γCD20) and introduced into a fused silica capillary (50 μm I.D. and 150 μm O.D., Polymicro Technologies, Phoenix, AZ, USA) by hydrodynamic injection at 12 kPa for 2 s. Then the capillary was then brought into a vial with separation buffer and MEKC was performed under a +400 V/cm electric field in a home-built instrument equipped with post-column LIF detection, previously described [88]. Fluorescence was selected with a 635 ± 27.5 nm filter (XF3015, Omega Optical, Brattleboro, VT, USA).

4.2.8. Data Analysis

In HPLC-LIF-MS, the MS detection of an eluting peak lagged 29±1 seconds relative to fluorescence detection. This time difference was used to associate MS and LIF signals. MS data were analyzed using DataAnalysis 4.0 supplied by Bruker Daltonics. When calculating chemical formula two restrictions were used: (i) the maximum number of nitrogen atoms in the chemical formula was set to two, and (ii) the mass tolerance was 20 ppm. Among these formulas, the selection of the best match was strongly dependent on its sigma value, which is an index of the deviations of observed from the predicted masses and intensities of monoisotopic peaks corresponding to given chemical formula. When using standard compounds, the formula with the lowest sigma value was the correct chemical composition. This, along with prior knowledge on doxorubicin metabolism, comparison of retention times with standards, and very low sigma values increased the confidence of the compounds' identifications. Fluorescence data for both HPLC-LIF-MS and MEKC-LIF experiments were analyzed using in house developed procedures in Igor Pro (WaveMetrics, Inc., Portland, OR) to calculate peak area. Concentrations of each compound were calculated from peak areas and plotted as a

function of time. The rates of consumption of doxorubicin and formation of the metabolites were determined from the data representing concentration versus time [84].

Concentrations were calculated based on fluorescence peak area and expressed as a mole fraction of doxorubicin at the onset of the metabolic reactions. The concentration of each metabolite was adjusted by its relative fluorescence quantum efficiency [84]. The total concentration of doxorubicin included both the concentrations of detected doxorubicin and doxorubicinone because the latter is produced from doxorubicin during the sample extraction procedure. Final concentrations of doxorubicin and its metabolites were determined from the plateaus observed at the end of a metabolic reaction. Maximum rates of reaction were measured at the onset of the metabolic reaction where concentrations are expected to vary linearly with time. The maximum rate of reaction of doxorubicin is negative because it was being consumed during the metabolic reaction). Box plots for statistical analysis were created using Igor Pro. Power analysis, t-tests and F-tests were performed using 'R' software (Free Software Foundation, Boston, MA).

4.3. Results

4.3.1. Separation and Identification of Doxorubicin and Metabolites

The HPLC-LIF-MS provided quantitative fluorescent data for the quantification of doxorubicin and metabolites and also structural mass spectrometry data in order to confirm the identity of the compounds observed by LIF. The compounds attributed to metabolism that were detected in the samples of both heart and liver were doxorubicin, 7-deoxydoxorubicinolone (Peak 2), and 7-deoxydoxorubicinone (Peak 4) (Figure 4-2B). Detection of a compound by MS lags that of the LIF detector due to added tubing

distance between the detectors. Doxorubicin elutes first (Figure 4-2C, Peak 1) followed by 7-deoxydoxorubicinolone (Figure 4-2C, Peak 2). The third peak is doxorubicinone (Figure 4-2C, Peak 3). This compound was not considered a metabolite because it is the result of acid hydrolysis during the extraction procedure. The fourth peak was determined to be 7-deoxydoxorubicinone (Figure 4-2C, Peak 4).

Separations using MEKC-LIF were used as an independent separation method to confirm observations of age-related changes in metabolism. In the parallel MEKC-LIF experiments, similar data was obtained for metabolism products. However, four metabolic products were observed (M1, M2, M3 and M4, Figure B-1, Appendix B). To identify metabolic compounds, standards of doxorubicinol and doxorubicinone were comigrated with the *in vitro* sample. Comigrations with the standard solutions suggest that the chemical structure of two of the metabolites may be similar to the standard compounds but not identical (i.e. the MEKC peaks only partially overlap). The intensities of the LIF signals corresponding to the observed metabolites (M1 and M2, Figure B-2, Appendix B) in MEKC-LIF follow a similar trend in concentration versus time as observed by HPLC-LIF-MS for 7-deoxydoxorubicinone and 7-deoxydoxorubicinolone (Figure B-2, Appendix B). M1 and M2 are assigned as 7-deoxydoxorubicinone and 7-deoxydoxorubicinolone respectively. M3 and M4 were not observed by HPLC-LIF-MS. This could be due to a difference in sample extraction procedure between the two methods or the compounds may be below the detection limit of HPLC-LIF-MS (LOD: 1×10^{-12} moles doxorubicin) yet detectable by MEKC-LIF (LOD: 6×10^{-20} moles doxorubicin).

4.3.2. Selection of Tissue for Aging Studies

The rate of doxorubicin consumption by the heart samples was significantly lower than that of the liver (Figure 4-3). Since our goal was to evaluate the feasibility of using HPLC-LIF-MS to assess changes in metabolism as a function of aging and both liver and heart produced the same compounds, we chose liver tissue for the age comparison studies. It is worth noting that the ratio of the concentrations of 7-deoxydoxorubicinone and 7-deoxydoxorubicinolone was significantly different between the two tissues. The concentration of 7-deoxydoxorubicinone was higher in the heart than in the liver, while the opposite was true for 7-deoxydoxorubicinolone (See Figure B-4, Appendix B).

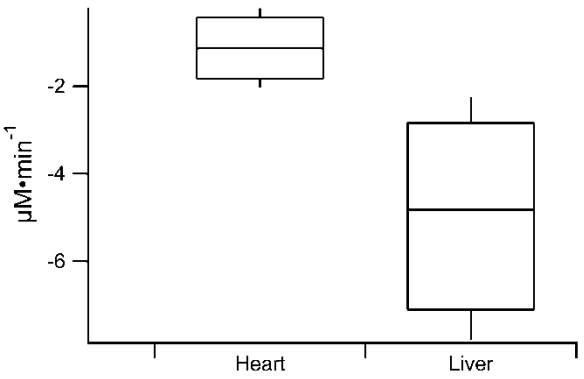

Figure 4-3. Rate of doxorubicin consumption by heart and liver tissues. Liver exhibits a much higher rate (n=4, $p<0.05$).

4.3.3. Metabolic Profiling

In the study of young adult versus old liver, addition of glucose-6-phosphate dehydrogenase to the PMF cocktail marked the onset of doxorubicin metabolism. Samples were taken at various time points and analyzed by HPLC-LIF-MS. The mole fraction of 7-deoxydorobucinone (triangles), 7-deoxydoxorubicinolone (squares), and doxorubicin (diamonds) relative to the initial amount of doxorubicin were plotted as a function of time (Figure 4-4A). From these plots, three metabolic parameters were compared for each detected compound between young and old: (i) the timeframe needed

to reach a steady state, maximum, or minimum concentration; (ii) the initial rate of biotransformation; and (iii) the final concentration.

The timeframe in which a compound reached a steady state, maximum, or minimum concentration is summarized in Figure 4-4B. For four young adult animals (filled markers), all maxima or minima occurred within 0-10 minutes. However, for the four old animals (blank markers), the timeframes are much more varied for the metabolites (i.e. up to 20-30 min. for 7-deoxydoxorubicinolone and up to 30-40 min for 7-deoxydoxorubicinone). This qualitative representation during which a given biotransformation is occurring indicates that all doxorubicin-related biotransformations in the PMF from the young adult liver (filled markers) occur within 10 minutes of the metabolic reaction. In contrast, the corresponding biotransformations in the PMF from the old liver (empty markers) occur in highly variable timeframes. It is important to bear in mind that these are *in vitro* biotransformations in which the enzymatic reactions conditions are experimentally controlled and maintained at maximum efficiency by the addition of cofactors. Thus, it is not surprising that the timeframes for *in vitro* experiments are shorter than pharmacokinetic studies of doxorubicin that would take ~ 8 hours [24]. Similar results were observed in the parallel MEKC-LIF experiments where doxorubicin was consumed rather quickly (e.g. 30 minutes). The metabolite M2 (Figure B-1, Appendix B) formed quickly which is consistent with its assignment as 7-deoxydoxorubicinolone.

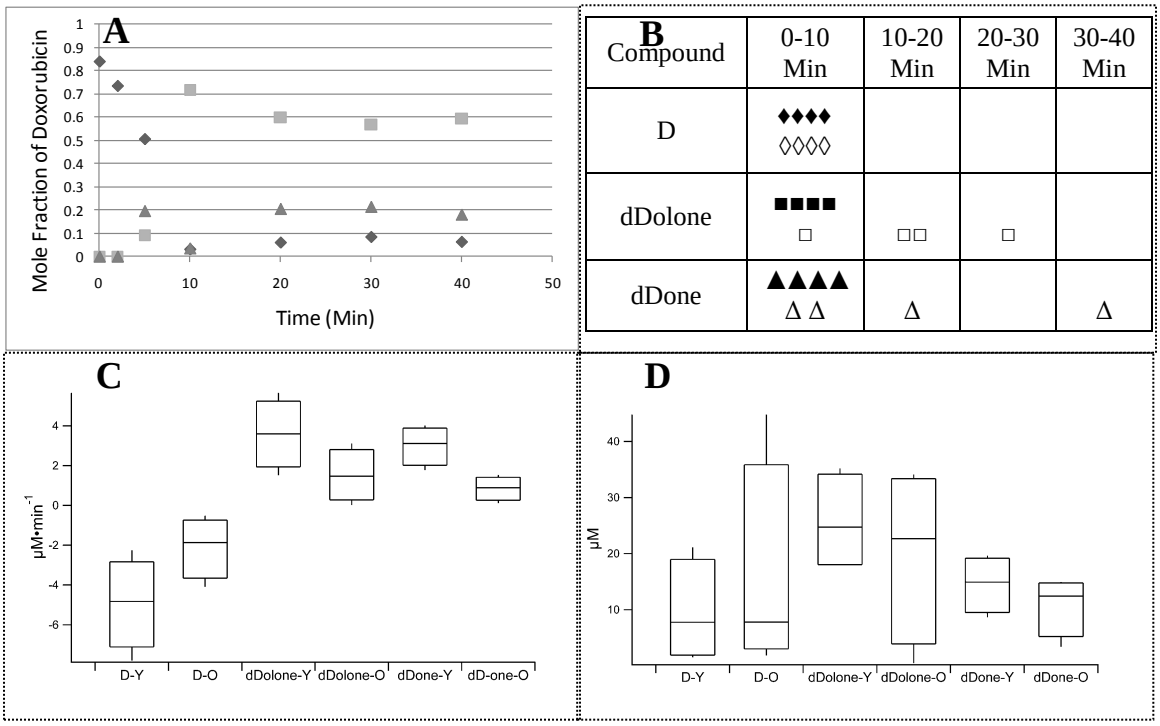

Figure 4-4. Biotransformation parameters of Dox in the PMF of young adult and old livers. The reaction mixture contained 5 mM magnesium chloride, 0.25 mM $NADP^+$, 2.5 mM glucose-6-phosphate, 50 μM doxorubicin and 2.0 units glucose-6-phosphate dehydrogenase. The solution was incubated at 37ºC in a heated mixer and samples taken at the indicated time points. Samples were extracted and analyzed by HPLC-LIF-MS. The fluorescence data was used for quantification. (A) Doxorubicin (diamonds), 7-deoxydoxorubicinolone (squares) and 7-deoxydoxorubicinone (triangles) expressed as a mole fraction of the initial amount of doxorubicin versus time. This data is representative of one young adult rat. (B) The timeframe required to reach a maximum, minimum or a steady state concentration. Solid symbols represent 1 young rat (10 months old) while empty symbols represent 1 old (26 months old) rat. (C) Initial rates of metabolic transformations. Four animals were included in each group. Rates between young and old animals for each compound are statistically different ($p<0.05$). D, dDolone, and dDone denote doxorubicin, 7-deoxydoxorubicinolone and 7-deoxydoxorubicinone, respectively. Y indicates young rats while O indicates old rats. (D) Final concentrations of compounds after metabolism. Four animals were included in each group. The concentrations between young and old animals for each compound were not statistically different ($p>0.15$).

The initial rate of biotransformation of a given compound is usually its maximum rate and it is related to the activities of the enzymes involved in the formation and biotransformation of such compound. Figure 4-4C shows the initial rate of consumption of doxorubicin (D-) 7-deoxydoxorubicinolone (dDolone-) and 7-deoxydoxorubicinone (dDone-) in the old (labeled with suffix "-O") and in the young adult (labeled with suffix "-Y") liver PMF. In all cases the rates of biotransformation were statistically lower ($p=0.5$) in the old than in the young adult liver PMF while their variances were not statistically significant. These findings were in perfect agreement with the results from parallel MEKC-LIF experiments (data not shown).

The final concentrations of compounds in the *in vitro* metabolic pool were measured in order to observe if the steady state concentration of one metabolite is favored differently with age. Neither the final average nor variance of the concentrations of each compound detected were not statistically different ($p > 0.15$) between the liver PMF of young adult and old animals (Figure 4-4D).

4.4. Discussion

Doxorubicin (Figure 4-1) is and has been a common treatment for carcinomas, sarcomas and lymphomas [10, 89] even in the elderly whose metabolism may be altered. The need for studying altered metabolism with age has led to the development of sensitive and customizable techniques to make the study of metabolic profiling more commonplace. The HPLC-LIF-MS methodologies presented here accomplished quantitative fluorescence data collection along with structural confirmation via mass spectrometry simultaneously. After method development, these methods can easily be transferred to instrumentation using only fluorescence detection to accomplish more

routine analyses. Chapter 3 describes the development of an HPLC-LIF-MS instrument and *in vitro* methodology to investigate the metabolic profile of doxorubicin from rat liver tissue [84]. Using this instrument, we were able to obtain simultaneously quantitative LIF data and structural MS data for identification of compounds. Two metabolic products were observed by HPLC-LIF-MS: 7-deoxydoxorubicinolone and 7-deoxydoxorubicinone (Figure 4-1 and 4-2). We also utilized, MEKC-LIF in order to confirm the HPLC-LIF-MS quantitative data and because of its superior sensitivity that is suitable to detect low abundance metabolic products. For instance, four metabolic compounds were observed (Figure B-1, Appendix B). While MEKC-LIF is a highly complementary technique, its separation buffers are incompatible with MS detection making it impossible to obtain direct structural identification of compounds.

Two important tissue types were examined: liver and heart. The liver is the main organ where detoxification and phase I metabolism occurs to remove xenobiotics from the body [13]. In the case of doxorubicin, the heart is of specific interest as cardiotoxic side-effects of the drug treatment have been reported and connected with a metabolic product, doxorubicinol (Figure 4-1). It was expected that doxorubicinol might be observed from heart tissue as that has been reported to be produced within the cytosol from heart tissue and attributed to cardiac damage during treatment with doxorubicin [10, 41]. This metabolite was not detected in the *in vitro* reactions using heart tissue, even when including dicumarol in the *in vitro* reactions. Since dicumarol inhibits NADPH-P450 reductase that is, in part, responsible for biotransformation of doxorubicin into the aglycone metabolites [29], we had anticipated that this inhibitor would result in a decrease in the formation of 7-deoxidoxorubicinolone even when doxorubicinol was not

observed, (i.e. left reaction pathway in Figure 1). Another consideration in selecting a tissue for the age comparison studies was that the rate of reaction of doxorubicin was significantly slower in heart tissue than liver tissue (Figure 4-3). Therefore, liver was used in the age comparison studies.

Since the expression of xenobiotic metabolizing enzymes (primarily CYP450 enzymes) has been observed to vary with age [4, 5, 22], three important parameters were monitored using the LIF detector of the HPLC-LIF-MS setup: the rate of biotransformation, the timeframe needed to reach a steady state concentration of a metabolic product, and the final steady state concentration of doxorubicin and its metabolic products. In this study we compared these metabolic parameters for each detected compound between young adult and old rats.

The timeframe required to reach a steady-state concentration of doxorubicin or its metabolic products varied between young adult and old rat liver PMF. In the young adult the maximum or minimum concentrations were reached within the first 10 minutes whereas in the old rats the timeframes were much more varied (Figure 4B). Some of the concentration maxima in old rats PMFs were reached as late as 30-40 minutes after the onset of the reaction. Monitoring the time needed to reach a steady-state concentration in an *in vivo* situation is extremely valuable in assessing biotransformations, investigate drug activation (e.g. prodrug), or assess cytotoxicity. The technology presented here could be easily extended to such *in vivo* studies applied to cohorts of animals in different age groups.

The initial maximum rate of biotransformation for doxorubicin, 7-deoxydoxorubicinolone and 7-deoxydoxorubicinone was always higher in young adult than old liver PMF (Figure 4C). Monitoring this parameter in *in vivo* studies would be extremely valuable since the rate of biotransformation is related to persistence of the drug and its metabolic products in the organ and is inversely related to the rate of elimination.

The final steady-state concentrations of doxorubicin and each of the two metabolites were not significantly different when comparing the young adult and old rat PMFs (Figure 4D). Since all samples are treated identically, a difference in the final concentration result may not be expected since the concentration of the metabolizing enzymes would only alter the rate of reaction.

Overall, this study introduces the use of HPLC-LIF-MS to describe differences in the rate of metabolism of doxorubicin between young adult and old animals. Even when these data are preliminary (i.e. 4 animals of each age were included), we determined that the initial rates of consumption of doxorubicin and rates of formation of 7-deoxydoxorubicinolone and 7-deoxydoxorubicinone are statistically different for young adult and old rat liver PMFs. A power analysis (80% power) of the data suggests that between 12 and 15 animals in each group are needed to determine if the end, steady state concentration are truly different between the adult young and old age groups.

4.5. Conclusion

The dual detection scheme of HPLC-LIF-MS made possible to identify doxorubicin metabolites and quantify various metabolic parameters (i.e. initial rate of reaction and final concentration) in metabolism occurring in the PMF taken from young

adult and old livers. These parameters are important to understanding a xenobiotic's pharmacokinetic properties such as the half-life, the clearance and the steady-state concentration of a given drug. The data here suggest that with aging the biotransformation of doxorubicin in rat liver slows down. Future work should use a larger cohort of animals and at least three ages [5]. Also, the age-related metabolic profile of doxorubicin in other tissue types and blood samples could be examined for metabolites not detected in these studies (i.e. doxorubicinol). Lastly, the future of the new methodologies presented here may see applications that investigate age-related changes in metabolism of drugs already in use, new compounds, and xenobiotics with health relevance (e.g. pesticides or environmental pollutants) in human specimens. This would aid in the understanding of the intricacies of age-related metabolic changes that will likely be associated with the ever increasingly complex medication regiments of the aging population.

Chapter 5

Conclusions and Future Work

5.1. Conclusions

The two main outcomes of this work are: (i) a new method useful for both identification and quantification of metabolic profiles of the fluorescent anti-cancer drug doxorubicin and (ii) application of this method to investigate the changes in the metabolism of doxorubicin with aging.

Using HPLC with tandem LIF and MS detectors allows the separation of doxorubicin and its metabolites, collection of quantitative fluorescent data and collection of structural mass spectrometry data. The separation is necessary to quantify doxorubicin and its fluorescent metabolites by LIF. LIF data is particularly useful to quantify each compound at different time points during *in vitro* metabolism experiments. On the other hand, MS data revealed that two metabolites, 7-deoxydoxorubicinone and 7-deoxydoxorubicinolone, are the most prominent metabolites in the *in vitro* metabolism of rat liver PMF. Doxorubicinol, one of the most common metabolites found in previous reports, was not observed.

The experiments presented in Chapter 4 show evidence of the applicability of HPLC-LIF-MS techniques to compare metabolism in biological systems. Specifically the analysis of liver PMF in two different age groups reveals that the activity responsible for the formation of 7-deoxydoxorubicinolone and 7-deoxydoxorubicinone decreases with increased age.

The results presented in Chapters 3 and 4 also pointed to some limitations. Only two prominent metabolites, 7-deoxydoxorubicinolone and 7-deoxydoxorubicinone, were detected and monitored using HPLC-LIF-MS. There may be other metabolites formed

that are either lost in the extraction procedure, not detected due to their low abundance, or not formed in the animal model chosen here. More than 10 peaks associated with doxorubicin metabolism after treatment with this drug have been observed using a more sensitive technique (MEKC-LIF) [37, 42, 43]. In the search for a suitable extraction procedure for sample cleanup, various methods were attempted (e.g. solid-phase extraction). The method chosen in Chapter 3 using perchloric acid was found to be efficient for extraction of doxorubicin and the observed metabolites. However, it may not be efficient for the extraction and analysis of all metabolites. Future adaptations of the work presented here are discussed in the next section.

5.2. Future Work

Based on the promises and limitations mentioned above, logical expansions to the current analytical procedures include: (i) improvement of detection limits by implementing capillary electrophoresis-mass spectrometry (CE-LIF-MS), more sensitive mass analyzers and nano-HPLC, (ii) application to other xenobiotics, (iii) analysis of other tissues and (iv) comparison of *in vitro* versus *in vivo* metabolism models. These are discussed below.

Implementing CE-LIF-MS technology may make a large improvement to the analysis of doxorubicin metabolism. Previously, the MEKC-LIF analysis of doxorubicin and metabolites showed more than 10 peaks (i.e. possible metabolites) [37, 42, 43]. By interfacing CE with tandem LIF and MS detectors, the improved detection limits of CE-LIF could be combined with structural determinations of the MS detector of suitable sensitivity. CE-MS is a promising approach combining the fast, biologically compatible separations of CE with MS capabilities for obtaining structural information to identify the

unknown metabolites [90]. The most common interface between CE and MS is an ESI source. Multiple advances have been made in recent years to make the ESI process from CE more efficient [90]. An interface for ESI without a sheath flow liquid would be ideal to reduce any additional dilution of the analytes. MEKC-MS can also be accomplished to separate successfully metabolite compounds prior to MS detection. Volatile surfactants, such as ammonium perfluorooctanoate [91]., have been used to form ESI compatible micelles to facilitate separations. Also, polymeric micelles of poly(sodium N-undecanoyl-L-leucinate) provided improved limits of detection in separations and provided enantioselective separation [92].

Nano-HPLC yields an improved limit of detection over μHPLC [93]. This is due to the reduced chromatographic dilution when using columns of increasingly small radius [33-35]. In many instances examining biomarkers and bioactive peptides, nano-HPLC has allowed detection limits in the mid to low pM range [93]. Nano-HPLC in combination with LIF and MS detection could provide a more sensitive analysis apparatus.

The use of more sensitive mass analyzers would improve the limit of detection for the mass spectrometer as well. Triple quadrupole mass analyzers have an increased sensitivity and can perform multiple reaction monitoring (MRM). However, they have a reduced mass resolution which is not adequate to identify truly unknown compounds [94, 95]. With increasingly efficient separations, narrow peaks from compounds become difficult to analyze due to the lengthened duty cycle. HPLC combined with triple quadrupole mass spectrometers are readily available commercially. CE separations have been combined with triple quadrupole instruments but there are few reports [96]. Matrix

assisted laser desorption (MALDI)-MS is an appealing technique to achieve lower limits of detection because one sample can be analyzed many times. However, this ionization technique is not readily amenable to interface with liquid separation techniques. Fractions of the separation must be collected on the MALDI matrix to be analyzed [97]. The Orbitrap mass analyzer (Thermo Scientific) has become a popular instrument in proteomics and metabolomics research [52, 98]. This mass analyzer has high mass resolution (~60,000) and a mass accuracy in the low ppm range, which are beneficial for the accurate identification of unknown compounds [52, 98]. The limits of detection are in the attomole to femtomole range [98]. While HPLC has been combined with the Orbitrap instrument [52], no reports for combining CE with an Orbitrap instrument are found.

Non-fluorescent compounds such as anticancer agents (e.g. mitoxantrone or paclitaxel) could be investigated using a UV-Vis detector in place of the LIF detector in the HPLC-LIF-MS instrument described here. This combination of HPLC-UV-MS has been accomplished previously [63, 64]. The added selectivity of fluorescence detection is lost. However, the benefit of the use of a tandem detector aids in the validation of separations of complex mixtures before more routine use with only a spectroscopic detector or mass spectrometer. This could lead to quicker development of routine separations in order to investigate a wider array of drugs.

Tandem detectors have great potential but more demonstrations of their use are needed. These detectors will find wide applicability in the analysis of human samples after exposure to xenobiotics, which is a daunting task given the estimate that people encounter 1-3 million xenobiotics in their lifetime and not all compounds are fluorescent [1, 2].

To completely understand a drug's or xenobiotic's fate upon entering the body, studies must be conducted taking into account all of the possible biochemical environments to be encountered by the foreign compound. The metabolic biotransformations of drugs and xenobiotics are expected to vary from tissue to tissue because of variations in the types and abundances of metabolizing enzymes associated with the tissue [8-10, 15, 41]. For example, the largest superfamily of xenobiotic metabolizing enzymes, CYP 450s, are differentially expressed amongst different organs. For example, the CYP450 enzymes of family 1 (involved in xenobiotic metabolism) are expressed differentially within the body. CYP1A1 is expressed primarily in extrahepatic tissues such as the lungs [3]. In contrast, CYP1A2 is expressed primarily in the liver with little if any detectable expression in the extrahepatic tissues [3]. Also, the small intestine contains a large number of CYP450s [9]. In the case of doxorubicin, the metabolite doxorubicinol has a dramatic effect on heart tissue (i.e. cardiotoxicity) [41]. Many other organs have also been investigated in rats including brain, kidney and pancreas for the presence of drug metabolites [62]. It is difficult to explore these organs in human subjects. Improvement of the necessary technologies to conduct the analysis on small tissue biopsies is the only likely possibility.

Doxorubicin's most accepted mechanism of action involves DNA intercalation [25, 41, 99]. Therefore, it is likely to find doxorubicin accumulating in the nucleus and mitochondria [38-40]. Metabolites in these environments may include DNA adducts [100]. To conduct experiments on specific organelles, it is necessary to conduct experiments on the specific subcellular fraction independent of all others. This involves fractionation steps such as differential centrifugation, gradient centrifugation and

immunoisolation [101]. If definitive conclusions are to be made about a specific organelle, research to obtain high purity organelle fractions must be completed.

There are gaps linking *in vitro* screening methods that are faster and provide a wealth of information to real world exposures [102]. A difference in metabolic products of doxorubicin was observed between perfused tissue and homogenized cells [103]. The conclusion was that the 7-deoxyaglycones are not part of the natural metabolism pathway of doxorubicin but result only under the conditions of the homogenized cells or tissue. This occurrence would explain the absence of previously reported metabolites, such as doxorubicinol, from *in vitro* studies of doxorubicin using homogenized tissue. Since the *in vitro* metabolism method presented in Chapter 3 did not detect doxorubicinol and only observed 7-deoxydoxorubicinolone and 7-deoxydoxorubicinone [84], the question arises as to how complete of a model *in vitro* metabolism can be. In order to address this question, rats could be treated *in vivo* with doxorubicin, the animals sacrificed and their livers removed. In parallel, the methods presented in Chapter 3 could be used to conduct *in vitro* experiments. The compared data would illustrate the completeness of the *in vitro* approach to *in vivo* treatments.

In summary, the development of HPLC-LIF-MS methodologies presented in this thesis provides a tool to be able to collect quantitative and structural data simultaneously to observe the metabolic profile of doxorubicin. This thesis work paves the way to the long term goal of improving technologies to monitor the metabolic profile of doxorubicin and other xenobiotics in biological samples. Particularly, application of this technology to aging-related metabolism of doxorubicin illustrates the potential of new technologies to

further our understanding of drug response, exposure, and metabolism with relation to age.

Bibliography

1. Idle, J. R.; Gonzalez, F. J. "Metabolomics." *Cell Metab.* **2007**, *6*, pp. 348-351.
2. Patterson, A. D.; Gonzalez, F. J.; Idle, J. R. "Xenobiotic metabolism: A view through the metabolometer." *Chem. Res. Toxicol.* **2010**, *23*, pp. 851-860.
3. Danielson, P. B. "The cytochrome p450 superfamily: Biochemistry, evolution and drug metabolism in humans." *Curr. Drug Metab.* **2002**, *3*, pp. 561-597.
4. Lee, J. S.; Ward, W. O.; Wolf, D. C.; Allen, J. W.; Mills, C.; DeVito, M. J.; Corton, J. C. "Coordinated changes in xenobiotic metabolizing enzyme gene expression in aging male rats." *Toxicol. Sci.* **2008**, *106*, pp. 263-283.
5. Sotaniemi, E.; Arranto, A.; Pelkonen, O.; Pasanen, M. "Age and cytochrome p450-linked drug metabolism in humans: An analysis of 226 subjects with equal histopathologic conditions." *Clin. Pharmacol. Ther.* **1997**, *61*, pp. 331-339.
6. Wauthier, V.; Verbeeck, R. K.; Calderon, B.; others. "The effect of ageing on cytochrome p450 enzymes: Consequences for drug biotransformation in the elderly." *Curr. Med. Chem.* **2007**, *14*, pp. 745–757-745–757.
7. Seymour, R. M.; Routledge, P. A. "Important drug-drug interactions in the elderly." *Drugs Aging* **1998**, *12*, pp. 485–494.
8. Forrest, G. L.; Gonzalez, B. "Carbonyl reductase." *Chem. Biol. Interact.* **2000**, *129*, pp. 21-40.
9. Kaminsky, L. S.; Fasco, M. J. "Small intestinal cytochromes p450." *Crit. Rev. Toxicol.* **1991**, *21*, pp. 407-422.
10. Licata, S.; Saponiero, A.; Mordente, A.; Minotti, G. "Doxorubicin metabolism and toxicity in human myocardium: Role of cytoplasmic deglycosidation and carbonyl reduction." *Chem. Res. Toxicol.* **2000**, *13*, pp. 414-420.
11. Coutts, R. T.; Su, P.; Baker, G. B. "Involvement of cyp2d6, cyp3a4, and other cytochrome p-450 isozymes in n-dealkylation reactions." *J. Pharmacol. Toxicol. Methods* **1994**, *31*, pp. 177-186.
12. Mohutsky, M. A.; Chien, J. Y.; Ring, B. J.; Wrighton, S. A. "Predictions of the in vivo clearance of drugs from rate of loss using human liver microsomes for phase i and phase ii biotransformations." *Pharm. Res.* **2006**, *23*, pp. 654-662.
13. Zeeh, J. "The aging liver: Consequences for drug treatment in old age." *Arch. Gerontol. Geriatr.* **2001**, *32*, pp. 255-263.
14. Nolin, T. D.; Naud, J.; Leblond, F. A.; Pichette, V. "Emerging evidence of the impact of kidney disease on drug metabolism and transport." *Clin. Pharmacol. Ther.* **2008**, *83*, pp. 898-903.
15. Colombo, T.; Donelli, M. G.; Urso, R.; Dallarda, S.; Bartosek, I.; Guaitani, A. "Doxorubicin toxicity and pharmacokinetics in old and young rats." *Exp. Gerontol.* **1989**, *24*, pp. 159-171.
16. Nelson, D. R.; Kamataki, T.; Waxman, D. J.; Guengerich, F. P.; Estabrook, R. W.; Feyereisen, R.; Gonzalez, F. J.; Coon, M. J.; Gunsalus, I. C.; Gotoh, O.; et al. "The p450 superfamily: Update on new sequences, gene mapping, accession numbers, early trivial names of enzymes, and nomenclature." *DNA Cell Biol.* **1993**, *12*, pp. 1-51.
17. Zordoky, B. N.; El-Kadi, A. O. "Induction of several cytochrome p450 genes by doxorubicin in h9c2 cells." *Vasc. Pharmacol.* **2008**, *49*, pp. 166-172.
18. *World population ageing 2009*; United Nations, 2009.

19. Kaufman, D. W.; Kelly, J. P.; Rosenberg, L.; Anderson, T. E.; Mitchell, A. A. "Recent patterns of medication use in the ambulatory adult population of the united states: The slone survey." *J. Am. Med. Assoc.* **2002**, *287*, pp. 337-344.
20. Dwyer, L. L.; Han, B.; Woodwell, D. A.; Rechtsteiner, E. A. "Polypharmacy in nursing home residents in the united states: Results of the 2004 national nursing home survey." *Am. J. Geriatr. Pharmacother.* **2010**, *8*, pp. 63-72.
21. Corsonello, A.; Pedone, C.; Incalzi, R. A. "Age-related pharmacokinetic and pharmacodynamic changes and related risk of adverse drug reactions." *Curr. Med. Chem.* **2010**, *17*, pp. 571-584.
22. Kiechel, J. R. "Biotransformation of drugs during aging." *Gerontology* **1982**, *28*, pp. 101-112.
23. Bolling, B. W.; Court, M. H.; Blumberg, J. B.; Chen, C. Y. O. "The kinetic basis for age-associated changes in quercetin and genistein glucuronidation by rat liver microsomes." *Journal of Nutritional Biochemistry* **2010**, *21*, pp. 498-503.
24. Bachur, N. R. "Adriamycin (nsc-123127) pharmacology." *Cancer Chemother. Rep.* **1975**, *6 (pt. 3)*, pp. 153-158.
25. Gewirtz, D. A. "A critical evaluation of the mechanisms of action proposed for the antitumor effects of the anthracycline antibiotics adriamycin and daunorubicin." *Biochem. Pharmacol.* **1999**, *57*, pp. 727-741.
26. Krohn, K. *Anthracyclines chemistry and biology*; Springer: Berlin, 2008.
27. Taatjes, D. J.; Gaudiano, G.; Resing, K.; Koch, T. H. "Redox pathway leading to the alkylation of DNA by the anthracycline, antitumor drugs adriamycin and daunomycin." *J. Med. Chem.* **1997**, *40*, pp. 1276–1286-1276–1286.
28. Takanashi, S.; Bachur, N. R. "Adriamycin metabolism in man. Evidence from urinary metabolites." *Drug Metab. Disposition* **1976**, *4*, pp. 79-87.
29. Tani, N.; Yabuki, M.; Komuro, S.; Kanamaru, H. "Characterization of the enzymes involved in the in vitro metabolism of amrubicin hydrochloride." *Xenobiotica* **2005**, *35*, pp. 1121-1133.
30. Horvath, C.; Melander, W.; Molnar, I. "Solvophobic interactions in liquid-chromatography with nonpolar stationary phases." *J. Chromatogr.* **1976**, *125*, pp. 129-156.
31. Dill, K. A. "The mechanism of solute retention in reversed-phase liquid chromatography." *J. Phys. Chem.* **1987**, *91*, pp. 1980-1988.
32. Dorsey, J. G.; Dill, K. A. "The molecular mechanism of retention in reversed-phase liquid chromatography." *Chem. Rev.* **1989**, *89*, pp. 331-346.
33. Chen, G. F.; Paces, M.; Marek, M.; Zhang, Y. K.; Seidel-Morgenstern, A.; Tallarek, U. "Dynamics of capillary electrochromatography: Experimental study of flow and transport in particulate beds." *Chem. Eng. Technol.* **2004**, *27*, pp. 417-428.
34. Karger, B. L.; Martin, M.; Guiochon, G. "Role of column parameters and injection volume on detection limits in liquid chromatography." *Anal. Chem.* **1974**, *46*, pp. 1640-1647.
35. Vissers, J. P. C. "Recent developments in microcolumn liquid chromatography." *J. Chromatogr.* **1999**, *856*, pp. 117–143-117–143.
36. Aaron, J. J.; Trajkovska, S. "Fluorescence studies of anti-cancer drugs - analytical and biomedical applications." *Curr. Drug Targets* **2006**, *7*, pp. 1067-1081.

37. Anderson, A. B.; Gergen, J.; Arriaga, E. A. "Detection of doxorubicin and metabolites in cell extracts and in single cells by capillary electrophoresis with laser-induced fluorescence detection." *J. Chromatogr. B* **2002**, *769*, pp. 97-106.
38. Beyer, U.; Rothen-Rutishauser, B.; Unger, C.; Wunderli-Allenspach, H.; Kratz, F. "Differences in the intracellular distribution of acid-sensitive doxorubicin-protein conjugates in comparison to free and liposomal formulated doxorubicin as shown by confocal microscopy." *Pharm. Res.* **2001**, *18*, pp. 29-38.
39. Coley, H. M.; Amos, W. B.; Twentyman, P. R.; Workman, P. "Examination by laser scanning confocal fluorescence imaging microscopy of the subcellular localisation of anthracyclines in parent and multidrug resistant cell lines." *Br. J. Cancer* **1993**, *67*, pp. 1316-1323.
40. Serrano, J.; Palmeira, C. M.; Kuehl, D. W.; Wallace, K. B. "Cardioselective and cumulative oxidation of mitochondrial DNA following subchronic doxorubicin administration." *Biochim. Biophys. Acta* **1999**, *1411*, pp. 201-205.
41. Minotti, G.; Licata, S.; Saponiero, A.; Menna, P.; Calafiore, A. M.; Di Giammarco, G.; Liberi, G.; Animati, F.; Cipollone, A.; Manzini, S.; Maggi, C. A. "Anthracycline metabolism and toxicity in human myocardium: Comparisons between doxorubicin, epirubicin, and a novel disaccharide analogue with a reduced level of formation and [4fe-4s] reactivity of its secondary alcohol metabolite." *Chem. Res. Toxicol.* **2000**, *13*, pp. 1336-1341.
42. Anderson, A. B.; Arriaga, E. A. "Subcellular metabolite profiles of the parent ccrf-cem and the derived cem/c2 cell lines after treatment with doxorubicin." *J. Chromatogr. B* **2004**, *808*, pp. 295-302.
43. Anderson, A. B.; Ciriacks, C. M.; Fuller, K. M.; Arriaga, E. A. "Distribution of zeptomole-abundant doxorubicin metabolites in subcellular fractions by capillary electrophoresis with laser-induced fluorescence detection." *Anal. Chem.* **2003**, *75*, pp. 8-15.
44. Andrews, P. A.; Brenner, D. E.; Chou, F. T.; Kubo, H.; Bachur, N. R. "Facile and definitive determination of human adriamycin and daunoribicin metabolites by high-pressure liquid chromatography." *Drug Metab. Disposition* **1980**, *8*, pp. 152-156.
45. Mross, K.; Maessen, P.; van der Vijgh, W. J.; Gall, H.; Boven, E.; Pinedo, H. M. "Pharmacokinetics and metabolism of epidoxorubicin and doxorubicin in humans." *J. Clin. Oncol.* **1988**, *6*, pp. 517-526.
46. El-Aneed, A.; Cohen, A.; Banoub, J. "Mass spectrometry, review of the basics: Electrospray, maldi, and commonly used mass analyzers." *Appl. Spectrosc. Rev.* **2009**, *44*, pp. 210-230.
47. Cech, N. B.; Enke, C. G. "Practical implications of some recent studies in electrospray ionization fundamentals." *Mass Spectrom. Rev.* **2001**, *20*, pp. 362-387.
48. Iribarne, J. V. "On the evaporation of small ions from charged droplets." *J. Chem. Phys.* **1976**, *64*, pp. 2287-2287.
49. Yamashita, M.; Fenn, J. B. "Electrospray ion source. Another variation on the free-jet theme." *J. Phys. Chem.* **1984**, *88*, pp. 4451–4459-4451–4459.

50. Binaschi, M.; Farinosi, R.; Borgnetto, M. E.; Capranico, G. "In vivo site specificity and human isoenzyme selectivity of two topoisomerase ii-poisoning anthracyclines." *Cancer Res.* **2000**, *60*, pp. 3770-3776.
51. Wieling, J. "Lc-ms-ms experiences with internal standards." *Chromatographia* **2002**, *55*, pp. 107-113.
52. Kamleh, A.; Barrett, M. P.; Wildridge, D.; Burchmore, R. J.; Scheltema, R. A.; Watson, D. G. "Metabolomic profiling using orbitrap fourier transform mass spectrometry with hydrophilic interaction chromatography: A method with wide applicability to analysis of biomolecules." *Rapid Commun. Mass Spectrom.* **2008**, *22*, pp. 1912-1918.
53. March, R. E. "Quadrupole ion traps." *Mass Spectrom. Rev.* **2009**, *28*, pp. 961-989.
54. Guilhaus, M.; Selby, D.; Mlynski, V. "Orthogonal acceleration time-of-flight mass spectrometry." *Mass Spectrom. Rev.* **2000**, *19*, pp. 65-107.
55. Wollnik, H. "Time-of-flight mass analyzers." *Mass Spectrom. Rev.* **1993**, *12*, pp. 89-114.
56. Leslie, A. D.; Volmer, D. A. "Dealing with the masses: A tutorial on accurate masses, mass uncertainties, and mass defects." *Spectroscopy* **2007**, *22*, pp. 32-39.
57. Lachatre, F.; Marquet, P.; Ragot, S.; Gaulier, J. M.; Cardot, P.; Dupuy, J. L. "Simultaneous determination of four anthracyclines and three metabolites in human serum by liquid chromatography-electrospray mass spectrometry." *J. Chromatogr. B* **2000**, *738*, pp. 281-291.
58. Liu, Y.; Yang, Y.; Liu, X.; Jiang, T. "Quantification of pegylated liposomal doxorubicin and doxorubicinol in rat plasma by liquid chromatography/electrospray tandem mass spectroscopy: Application to preclinical pharmacokinetic studies." *Talanta* **2008**, *74*, pp. 887-895.
59. Takanashi, S.; Bachur, N. R. "Daunorubicin metabolites in human urine." *J. Pharmacol. Exp. Ther.* **1975**, *195*, pp. 41-49.
60. Arnold, R. D.; Slack, J. E.; Straubinger, R. M. "Quantification of doxorubicin and metabolites in rat plasma and small volume tissue samples by liquid chromatography/electrospray tandem mass spectroscopy." *J. Chromatogr. B* **2004**, *808*, pp. 141-152.
61. Badea, I.; Lazar, L.; Moja, D.; Nicolescu, D.; Tudose, A. "A hplc method for the simultaneous determination of seven anthracyclines." *J. Pharm. Biomed. Anal.* **2005**, *39*, pp. 305-309.
62. Urva, S. R.; Shin, B. S.; Yang, V. C.; Balthasar, J. P. "Sensitive high performance liquid chromatographic assay for assessment of doxorubicin pharmacokinetics in mouse plasma and tissues." *J. Chromatogr. B* **2009**, *877*, pp. 837-841.
63. Crow, F. W.; Cragun, J. D.; Johnson, K. L.; Ruiz, M. V.; Posada De La Paz, M.; Naylor, S. "On-line hplc-uv-mass spectrometry and tandem mass spectrometry for the rapid delineation and characterization of differences in complex mixtures: A case study using toxic oil variants." *Biomed. Chromatogr.* **2002**, *16*, pp. 311-318.
64. Akbay, C.; Rizvi, S. A.; Shamsi, S. A. "Simultaneous enantioseparation and tandem uv-ms detection of eight beta-blockers in micellar electrokinetic chromatography using a chiral molecular micelle." *Anal. Chem.* **2005**, *77*, pp. 1672-1683.

65. Huhn, C.; Neususs, C.; Pelzing, M.; Pyell, U.; Mannhardt, J.; Putz, M. "Capillary electrophoresis-laser induced fluorescence-electrospray ionization-mass spectrometry: A case study." *Electrophoresis* **2005**, *26*, pp. 1389-1397.
66. Gennaro, L. A.; Salas-Solano, O. "On-line ce-lif-ms technology for the direct characterization of n-linked glycans from therapeutic antibodies." *Anal. Chem.* **2008**, *80*, pp. 3838-3845.
67. Coleman, S.; Liu, S. M.; Linderman, R.; Hodgson, E.; Rose, R. L. "In vitro metabolism of alachlor by human liver microsomes and human cytochrome p450 isoforms." *Chem. Biol. Interact.* **1999**, *122*, pp. 27-39.
68. Sheets, J. J.; Schmidt, A.; Samaritoni, J. G.; Gifford, J. M. "In vitro metabolism of the n-alkyl-n-(5-isothiazolyl)- and n-(alkylisothiazolin-5-ylidene)phenylacetamides. Evidence of proinsecticidal activity." *J. Agric. Food Chem.* **1997**, *45*, pp. 4826-4832.
69. Golay, M. J. E. In *Gas chromatography, 1958*; Hesty, D. H., Ed.; Academic Press: New York, 1958, pp 36.
70. Sternberg, J. C. "Extracolumn contributions to chromatographic band broadening." *Advances in Chromatography* **1966**, *2*, pp. 205-270.
71. Licata, S.; Saponiero, A.; Mordente, A.; Minotti, G. "Doxorubicin metabolism and toxicity in human myocardium: Role of cytoplasmic deglycosidation and carbonyl reduction." *Chem. Res. Toxicol.* **2000**, *13*, pp. 414-420.
72. Colombo, T.; Donelli, M. G.; Urso, R.; Dallarda, S.; Bartosek, I.; Guaitani, A. "Doxorubicin toxicity and pharmacokinetics in old and young rats." *Exp. Gerontol.* **1989**, *24*, pp. 159-171.
73. Lachatre, F.; Marquet, P.; Ragot, S.; Gaulier, J. M.; Cardot, P.; Dupuy, J. L. "Simultaneous determination of four anthracyclines and three metabolites in human serum by liquid chromatography-electrospray mass spectrometry." *J. Chrmatogr., B: Anal. Technol. Biomed. Life Sci.* **2000**, *738*, pp. 281-291.
74. Minotti, G.; Licata, S.; Saponiero, A.; Menna, P.; Calafiore, A. M.; Di Giammarco, G.; Liberi, G.; Animati, F.; Cipollone, A.; Manzini, S.; Maggi, C. A. "Anthracycline metabolism and toxicity in human myocardium: Comparisons between doxorubicin, epirubicin, and a novel disaccharide analogue with a reduced level of formation and [4fe-4s] reactivity of its secondary alcohol metabolite." *Chem. Res. Toxicol.* **2000**, *13*, pp. 1336-1341.
75. Takanashi, S.; Bachur, N. R. "Daunorubicin metabolites in human urine." *J. Pharmacol. Exp. Ther.* **1975**, *195*, pp. 41-49.
76. Minotti, G.; Menna, P.; Salvatorelli, E.; Cairo, G.; Gianni, L. "Anthracyclines: Molecular advances and pharmacologic developments in antitumor activity and cardiotoxicity." *Pharmacological reviews* **2004**, *56*, pp. 185-229.
77. Singh, K. K.; Russell, J.; Sigala, B.; Zhang, Y.; Williams, J.; Keshav, K. F. "Mitochondrial DNA determines the cellular response to cancer therapeutic agents." *Oncogene* **1999**, *18*, pp. 6641-6646.
78. Sokolove, P. M. "Oxidation of mitochondrial pyridine nucleotides by aglycone derivatives of adriamycin." *Arch. Biochem. Biophys.* **1991**, *284*, pp. 292-297.
79. Sokolove, P. M. "Interactions of adriamycin aglycones with mitochondria may mediate adriamycin cardiotoxicity." *Int. J. Biochem.* **1994**, *26*, pp. 1341-1350.

80. Nolin, T. D.; Naud, J.; Leblond, F. A.; Pichette, V. "Emerging evidence of the impact of kidney disease on drug metabolism and transport." *Clinical pharmacology and therapeutics* **2008**, *83*, pp. 898-903.
81. Gennaro, L. A.; Salas-Solano, O. "On-line ce-lif-ms technology for the direct characterization of n-linked glycans from therapeutic antibodies." *Analytical chemistry* **2008**, *80*, pp. 3838-3845.
82. Anderson, A. B.; Arriaga, E. A. "Subcellular metabolite profiles of the parent ccrf-cem and the derived cem/c2 cell lines after treatment with doxorubicin." *J. Chromatogr. B Analyt. Technol. Biomed. Life Sci.* **2004**, *808*, pp. 295-302.
83. Andrews, P. A.; Brenner, D. E.; Chou, F. T.; Kubo, H.; Bachur, N. R. "Facile and definitive determination of human adriamycin and daunoribicin metabolites by high-pressure liquid chromatography." *Drug metabolism and disposition: the biological fate of chemicals* **1980**, *8*, pp. 152-156.
84. Katzenmeyer, J. B.; Eddy, C. V.; Arriaga, E. A. "Tandem laser-induced fluorescence and mass spectrometry detection for high-performance liquid chromatography analysis of the in vitro metabolism of doxorubicin." *Anal. Chem.* **2010**, *In Press*.
85. Coleman, S.; Liu, S.; Linderman, R.; Hodgson, E.; Rose, R. L. "In vitro metabolism of alachlor by human liver microsomes and human cytochrome p450 isoforms." *Chemico-biological interactions* **1999**, *122*, pp. 27-39.
86. Sheets, J. J.; Schmidt, A.; Samaritoni, J. G.; Gifford, J. M. "In vitro metabolism of the n-alkyl-n-(5-isothiazolyl)- and n-(alkylisothiazolin-5-ylidene)phenylacetamides. Evidence of proinsecticidal activity." *J. Agric. Food Chem.* **1997**, *45*, pp. 4826-4832.
87. Urva, S. R.; Shin, B. S.; Yang, V. C.; Balthasar, J. P. "Sensitive high performance liquid chromatographic assay for assessment of doxorubicin pharmacokinetics in mouse plasma and tissues." *J. Chromatogr. B Analyt. Technol. Biomed. Life Sci.* **2009**, *877*, pp. 837-841.
88. Duffy, C. F.; Gafoor, S.; Richards, D. P.; Admadzadeh, H.; O'Kennedy, R.; Arriaga, E. A. "Determination of properties of individual liposomes by capillary electrophoresis with postocolumn laser-induced fluorescence detection." *Anal. Chem.* **2001**, *73*, pp. 1855-1861.
89. Blum, R. H.; Carter, S. K. "Adriamycin. A new anticancer drug with significant clinical activity." *Ann. Intern. Med.* **1974**, *80*, pp. 249-259.
90. Kostal, V.; Katzenmeyer, J.; Arriaga, E. A. "Capillary electrophoresis in bioanalysis." *Anal. Chem.* **2008**, *80*, pp. 4533-4550.
91. Van Biesen, G.; Bottaro, C. S. "Ammonium perfluorooctanoate as a volatile surfactant for the analysis of n-methylcarbamates by mekc-esi-ms." *Electrophoresis* **2006**, *27*, pp. 4456-4468.
92. Hou, J. G.; Rizvi, S. A. A.; Zheng, J.; Shamsi, S. A. "Application of polymeric surfactants in micellar electrokinetic chromatography-electrospray ionization mass spectrometry of benzodiazepines and benzoxazocine chiral drugs." *Electrophoresis* **2006**, *27*, pp. 1263-1275.
93. Saz, J. M.; Marina, M. L. "Application of micro- and nano-hplc to the determination and characterization of bioactive and biomarker peptides." *J. Sep. Sci.* **2008**, *31*, pp. 446-458.

94. Glish, G. L.; Burinsky, D. J. "Hybrid mass spectrometers for tandem mass spectrometry." *J. Am. Soc. Mass Spectrom.* **2008**, *19*, pp. 161-172.
95. Lu, W.; Bennett, B. D.; Rabinowitz, J. D. "Analytical strategies for lc-ms-based targeted metabolomics." *Journal of Chromatography B-Analytical Technologies in the Biomedical and Life Sciences* **2008**, *871*, pp. 236-242.
96. Dunayevskiy, Y. M.; Vouros, P.; Wintner, E. A.; Shipps, G. W.; Carell, T.; Rebek, J. "Application of capillary electrophoresis electrospray ionization mass spectrometry in the determination of molecular diversity." *Proc. Natl. Acad. Sci. U. S. A.* **1996**, *93*, pp. 6152-6157.
97. Zhang, B. Y.; McDonald, C.; Li, L. "Combining liquid chromatography with maldi mass spectrometry using a heated droplet interface." *Anal. Chem.* **2004**, *76*, pp. 992-1001.
98. Macek, B.; Waanders, L. F.; Olsen, J. V.; Mann, M. "Top-down protein sequencing and ms3 on a hybrid linear quadrupole ion trap-orbitrap mass spectrometer." *Mol. Cell. Proteomics* **2006**, *5*, pp. 949-958.
99. Arcamone, F. *Doxorubicin : Anticancer antibiotics*; Academic Press: New York, 1981.
100. Wang, A. H.; Gao, Y. G.; Liaw, Y. C.; Li, Y. K. "Formaldehyde cross-links daunorubicin and DNA efficiently: Hplc and x-ray diffraction studies." *Biochemistry (Mosc).* **1991**, *30*, pp. 3812-3815.
101. Pasquali, C.; Fialka, I.; Huber, L. A. "Subcellular fractionation, electromigration analysis and mapping of organelles." *Journal of Chromatography B: Biomedical Sciences and Applications* **1999**, *722*, pp. 89–102-189–102.
102. Cohen Hubal, E. A.; Richard, A.; Aylward, L.; Edwards, S.; Gallagher, J.; Goldsmith, M. R.; Isukapalli, S.; Tornero-Velez, R.; Weber, E.; Kavlock, R. "Advancing exposure characterization for chemical evaluation and risk assessment." *J. Toxicol. Environ. Health* **2010**, *13*, pp. 299-313.
103. Vrignaud, P.; Londosgagliardi, D.; Robert, J. "Hepatic-metabolism of doxorubicin in mice and rats." *Eur. J. Drug Metab. Pharmacokinet.* **1986**, *11*, pp. 101-105.
104. Heijn, M.; Roberge, S.; Jain, R. K. "Cellular membrane permeability of anthracyclines does not correlate with their delivery in a tissue-isolated tumor." *Cancer Res.* **1999**, *59*, pp. 4458-4463.

Appendix A

Supplementary Material for Chapter 3

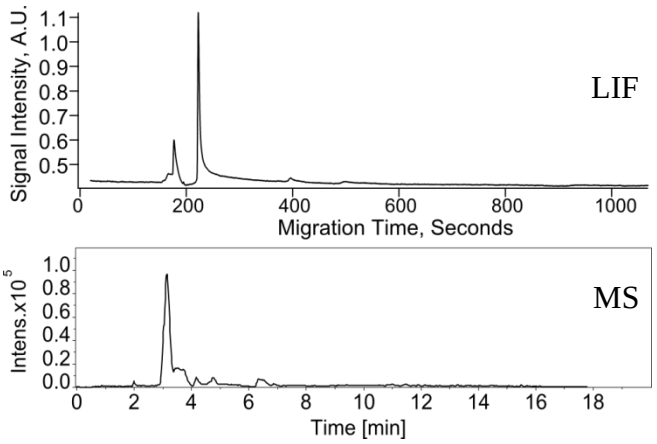

Figure A-1. LIF and MS detection of a PMF sample that was not treated with doxorubicin. Liver PMF was extracted as described in the experimental section of the main manuscript. No doxorubicin treatment was applied. Signals observed correspond to compounds in the PMF matrix.

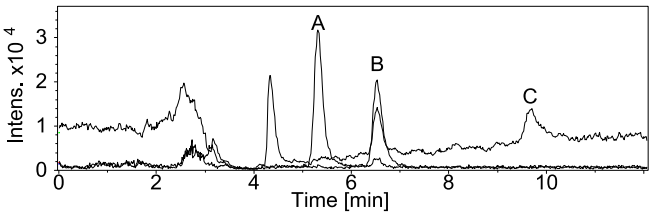

Figure A-2. Doxorubicinol can be extracted and detected using HPLC-LIF-MS. Overlayed extracted ion chromatograms for doxorubicinol (Peak A, m/z 546.2), doxorubicin (Peak B, m/z 544.2) and doxorubicinone (Peak C, m/z 397.2). A mixture of liver PMF, 10 µM doxorubicinol, 10 µM doxorubicin and 10 µM doxorubicinone was prepared, extracted and analyzed using the methods described in the experimental section (Chapter 3.2). All three compounds are detectable by mass spectrometry.

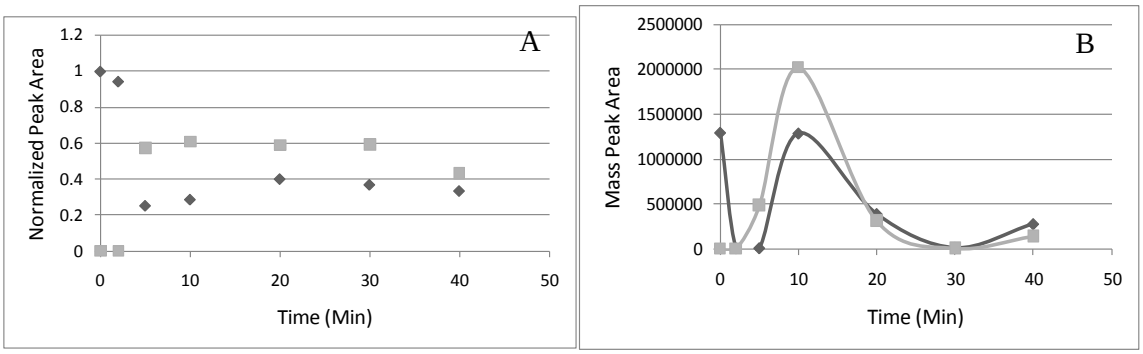

Figure A-3. Sample–to–sample variability in ion intensities demonstrating that MS is not suitable for quantitation. (A) LIF peak areas for doxorubicin (diamonds) and 7-deoxydoxorubicinolone (squares) at various times in the metabolic reaction. (B) MS peak areas for the same compounds and time points shown in (A). While LIF detection show well-defined trends in metabolic changes as function of time, MS detection is affected by ionization conditions that results in highly variable signals that complicate the determination of metabolic changes as a function of time.

Calculation diffusion broadening of peaks caused by the tubing connecting the HPLC system and the ESI interface.

The travel time between the LIF and MS detectors (i.e. t = 29 s) results in longitudinal diffusion that may contribute to the difference in peak efficiency observed between these two detectors. The variance due to longitudinal diffusion (σ^2_{diff}) of a compound in solution during its travel time (t) in an open tube is

$$\sigma^2_{diff} = 2Dt \qquad \text{Equation A-1}$$

where D is its diffusion coefficient (D ~ 2×10^{-6} cm^2/s [104]*)*. Thus σ^2_{diff}~5.8×10^{-5} cm^2. Conversion to the time domain using the linear velocity (0.52 cm/s) gives 2.1×10^{-4} s^2, which is needed to compare it with the variance observed by the LIF detector (σ^2_{LIF}), which is calculated as

$$\sigma^2_{LIF} = \frac{t^2_{LIF}}{N_{LIF}} \qquad \text{Equation A-2}$$

where t_{LIF} and N_{LIF} are the retention time and theoretical plates determined by the LIF detector. Using the values given in Table 3-1, σ^2_{LIF} = 7.6 s^2

Thus, expected additional broadening due to the separation between the two detectors is

$$\frac{\sigma^2_{diff}}{\sigma^2_{LIF}} = 2.7\times10^{-5} \qquad \text{Equation A-3}$$

Compared to the difference in variances observed by the two detectors,

$$\sigma_{MS}^2 - \sigma_{LIF}^2 = \frac{t_{MS}^2}{N_{MS}} - \frac{t_{LIF}^2}{N_{LIF}} = 29.47 s^2 \qquad \text{Equation A-4}$$

σ_{diff}^2 accounts for only 0.0007% of the observed increase in peak broadening. Other factors (e.g. ESI interface) are more likely to explain the differences in peak efficiencies between the two detectors.

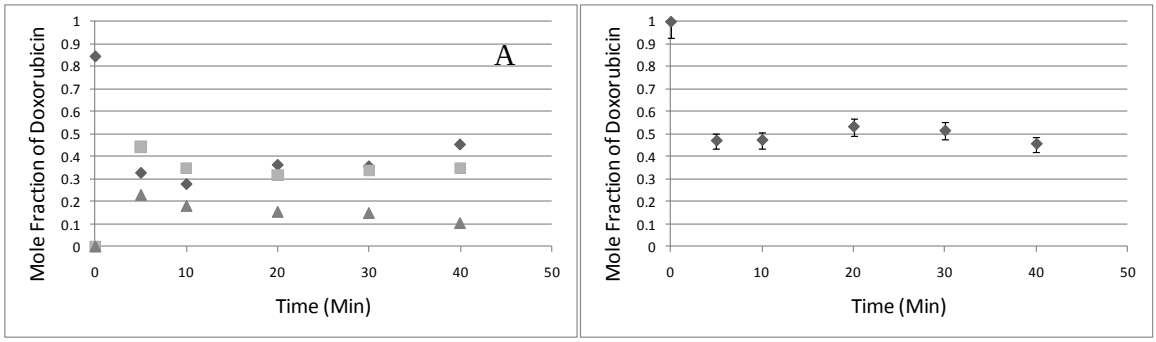

Figure A-4. Metabolite profiles as a function of reaction time. (A) shows data from Figure 5C. Doxorubicin is represented by diamonds. (B) shows doxorubicin plus doxorubicinone mole fractions. Error bars in B represent 7.5% error in LIF determinations observed using standards of doxorubicin. The increase in doxorubicin concentration in late reaction times (i.e. longer than 20 minutes) is accounted for in the variability of acid hydrolysis in the perchloric acid extraction.

Appendix B

Supplementary Material for Chapter 4

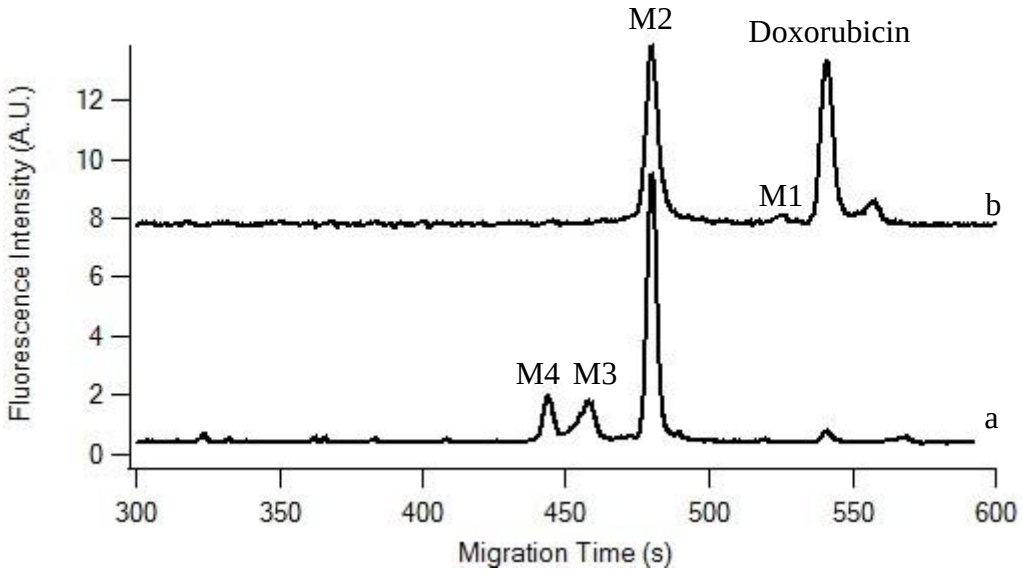

Figure B-1. MEKC-LIF analysis of the in vitro metabolism of Dox in post-mitochondria fractions of young and old rat livers. Electropherograms show Dox and metabolites after 2 h incubation of Dox in (a) young rat liver and (b) old rat liver. Trace b is y offset for clarity. Young and old samples were diluted 25 and 50 times in separation buffer, respectively before analysis. Separations were performed in a 45 cm (trace a) or 45.8 cm (trace b) long, 50 µm i.d. fused silica capillary at 400 V/cm in BS50-γCD20 buffer. Migration times were corrected for the difference in capillary length. Analytes were excited at 488 nm and fluorescence was detected at 635 ± 27.5 nm.

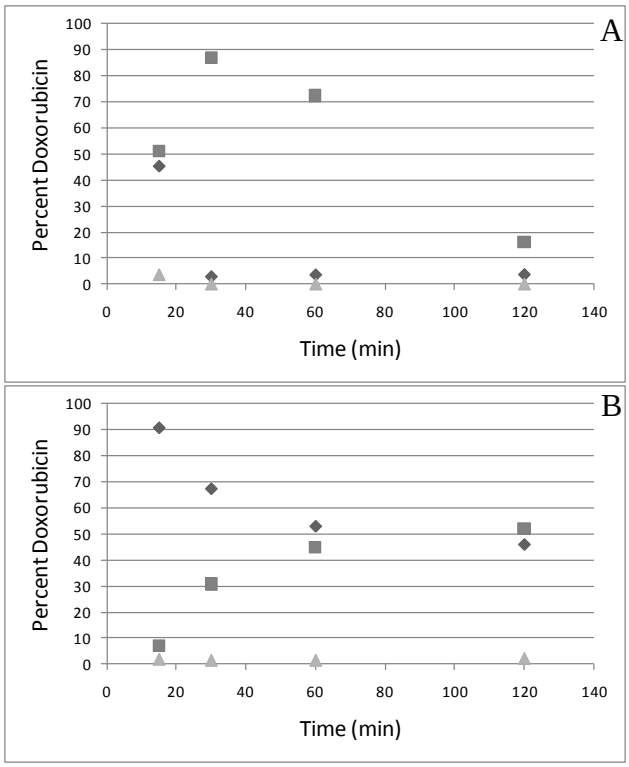

Figure B-2. Doxorubicin and metabolites changing with time in post-mitochondria fraction of young and old rat liver. (A) is data from a 10 months old rat. (B) is data from a 26 months old rat. Values are expressed as a percentage of doxorubicin peak area. Doxorubicin is represented by diamonds, 7-deoxydoxorubicinolone is represented by squares and 7-deoxydoxorubicinone is represented by triangles.

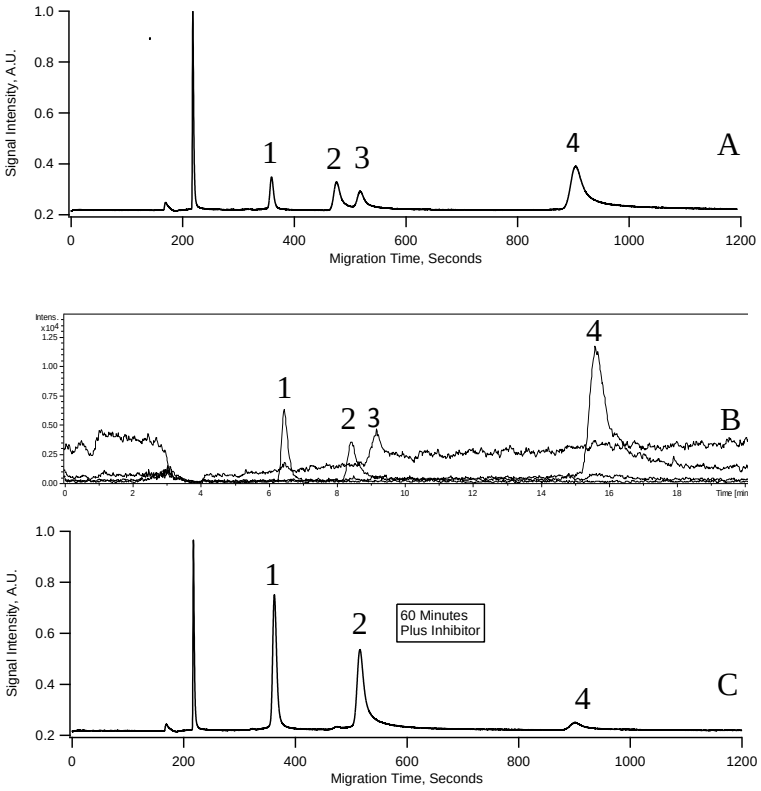

Figure B-3. Doxorubicin metabolism in heart tissue in the presence and absence of dicumarol. (A) LIF chromatogram show the expected peaks: doxorubicin (Peak 1), 7-deoxydoxorubicinolone (Peak 2), doxorubicinone (Peak 3) and 7-deoxydoxorubicinone (Peak 4). (B) MS confirmed the identity of these peaks by monitoring the extracted ion current for each of these peaks [84]. No doxorubicinol was observed. (C) In the presence of dicumarol, 7-deoxydoxorubicinolone and 7-deoxydoxorubicinone are less abundant. No doxorubicinol was observed. Incubation time 60 minutes. Other conditions are described in Chapter 4.2.

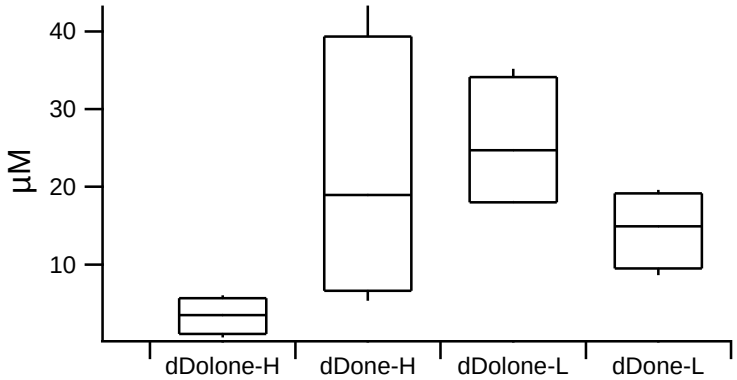

Figure B-4. Comparison of concentrations of 7-deoxydoxorubicinolone (dDolone) and 7-deoxydoxorubicinone (dDone) resulting from incubation of doxorubicin *in vitro* in liver and heart tissue. H indicates analysis of heart tissue; L indicates analysis of liver tissue. dDone was at a significantly higher concentration than dDolone in heart tissue The opposite is true for liver tissue. (n=4).